Further Studies of the Seismic Characteristics of Russian Explosions in Cavities: Implications For Cavity Decoupling of Underground Nuclear Explosions

J. R. Murphy
I. O. Kitov
N. Rimer
D. D. Sultanov
B. W. Barker
J. L. Stevens
V. V. Adushkin
K. H. Lie

Maxwell Laboratories, Incorporated
S-CUBED Division
P. O. Box 1620
La Jolla, CA 92038-1620

January, 1996

Final Report
August 1993 - November 1995

19960401 071

PHILLIPS LABORATORY
Directorate of Geophysics
AIR FORCE MATERIEL COMMAND
HANSCOM AFB, MA 01731-3010

This technical report has been reviewed and is approved for publication.

_____
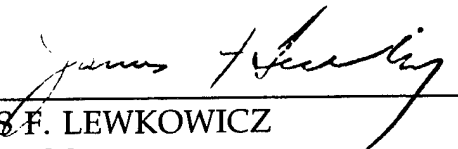
JAMES F. LEWKOWICZ
Contract Manager
Earth Sciences Division

_____

JAMES F. LEWKOWICZ
Director
Earth Sciences Division

REPORT DOCUMENTATION PAGE

1. AGENCY USE ONLY (Leave blank)	2. REPORT DATE	3. REPORT TYPE AND DATES COVERED
	January 1996	Final August 1993–November 1995

4. TITLE AND SUBTITLE
FURTHER STUDIES OF THE SEISMIC CHARACTERISTICS OF RUSSIAN EXPLOSIONS IN CAVITIES: IMPLICATIONS FOR CAVITY DECOUPLING OF UNDERGROUND NUCLEAR EXPLOSIONS

6. AUTHOR(S)
J. R. Murphy, I. O. Kitov*, N. Rimer, D. D. Sultanov*, B. W. Barker, J. L. Stevens, V. V. Adushkin, K. H. Lie

5. FUNDING NUMBERS
Contract:
F19628-93-C-0126

PE 62301E
PR NM93 TA GM
WU AJ

7. PERFORMING ORGANIZATION NAME(S) AND ADDRESS(ES)
Maxwell Laboratories, Inc.
S-CUBED Division
P.O. Box 1620
La Jolla, CA 92038-1620

8. PERFORMING ORGANIZATION REPORT NUMBER
SSS-FR-96-15265

9. SPONSORING/MONITORING AGENCY NAME(S) AND ADDRESS(ES)
Phillips Laboratory
29 Randolph Road
Hanscom AFB, MA 01731-3010

Contract Manager: James F. Lewkowicz/GPE

10. SPONSORING/MONITORING AGENCY REPORT NUMBER
PL-TR-96-2017

11. SUPPLEMENTARY NOTES

* Institute for Dynamics of the Geospheres, Russian Academy of Sciences

12a. DISTRIBUTION/AVAILABILITY STATEMENT

Approved for public release; distribution unlimited

12b. DISTRIBUTION CODE

13. ABSTRACT (Maximum 200 words)
This report provides a summary of the results of a joint research program under which scientists from S-CUBED have been working with scientists from the Russian Institute for Dynamics of the Geospheres in an attempt to develop a better understanding of the effects of cavity decoupling on the seismic signals produced by underground nuclear explosions. Investigations conducted under this program have focused on analyses of seismic data recorded from a series of HE cavity decoupling experiments conducted by the Russians in Kirghizia in 1960, and from a sequence of nuclear tests conducted in a water-filled cavity at the Soviet Azgir test site during the period 1975-1979. The Kirghizia series included tests designed to assess the influence of cavity geometry on decoupling effectiveness, and comparisons of near-field seismic data recorded from these tests indicate that the low frequency decoupling factor is independent of cavity shape for elongated cavities with length to width ratios of 6 or more, in agreement with previous theoretical simulation results. Broadband seismic data recorded from the Azgir water-filled cavity tests are analyzed to estimate cavity/tamped source spectral ratios, and the results are compared with theoretical finite difference simulations of these tests.

14. SUBJECT TERMS

Seismic	Explosion	Kirghizia	Nuclear
Cavity Decoupling	HE	Azgir	CTBT

15. NUMBER OF PAGES
80

16. PRICE CODE

17. SECURITY CLASSIFICATION OF REPORT	18. SECURITY CLASSIFICATION OF THIS PAGE	19. SECURITY CLASSIFICATION OF ABSTRACT	20. LIMITATION OF ABSTRACT
UNCLASSIFIED	UNCLASSIFIED	UNCLASSIFIED	UNLIMITED

Table of Contents

List of Illustrations

iv

vi

1. INTRODUCTION

The cavity decoupling evasion scenario continues to represent the greatest challenge to effective seismic monitoring of any eventual Comprehensive Test Ban Treaty (CTBT). However, despite the fact that the feasibility of this evasion concept was experimentally established nearly 30 years ago by the U.S. STERLING nuclear cavity decoupling test, a number of issues of importance with respect to seismic monitoring still remain unresolved. This is the case because the available experimental database is too sparse and uncertain to provide a firm basis for resolving these questions, and because the theoretical models being used to simulate the seismic source characteristics of such tests are strongly dependent on the still uncertain low pressure equations of state used to represent the response of real earth materials to explosive loading (Murphy *et al.*, 1996). As a result, significant uncertainty is associated with extrapolations to cavity decoupling test conditions which are outside the range of previous experience.

From a practical perspective, the principal uncertainties relate to the assessment of the effects of cavity size and shape on decoupling effectiveness. That is, because the spherical cavity sizes required for theoretically "full" decoupling in the yield range of potential testing interest are so large and difficult to construct (Murphy, 1980), there is a significant incentive for a clandestine tester to quantitatively evaluate the penalties associated with using progressively smaller cavities and elongated cavities which are nonspherical in shape. Over the past several years, we at S-CUBED have been carrying out a wide range of nonlinear, finite difference simulations of cavity decoupling in which the effects of cavity size and shape have been analyzed for both nuclear and chemical explosions in various source media (Murphy *et al.*, 1988; Stevens *et al.*, 1991a, 1991b; Rimer *et al.*, 1994; Murphy *et al.*, 1996). While the results of these simulations have been very informative, it has been difficult to critically assess their fidelity, because of the limited U.S. experimental database on cavity decoupling. However, scientists from the Institute for Dynamics of the Geospheres (IDG) of the Russian Academy of Sciences have recently

begun publishing new information on some Russian decoupling experiments (e.g., Adushkin *et al.*, 1992) which provide data relevant to these issues. For this reason, S-CUBED and IDG scientists initiated a joint research investigation in which an attempt has been made to integrate these newly available data and theoretical results in order to develop an improved, quantitative capability for evaluating the plausibility of various cavity decoupling evasion scenarios.

The research results summarized in this report have centered on a comprehensive analysis of seismic data recorded from a series of HE cavity decoupling experiments conducted by the Russians in Kirghizia in 1960 and on the analysis of data recorded from a series of nuclear tests conducted in a water-filled cavity at the Soviet Azgir test site in the 1975-1979 time frame. The map locations of these two test sites within the territories of the former Soviet Union are shown in Figure 1. Data recorded from the Kirghizia tests in cavities of different size and shape in limestone are compared and analyzed in Section 2, where they are also evaluated in terms of the results of theoretical, finite difference simulations of tamped and cavity decoupled explosions in this source medium. This is followed in Section 3 by an analysis of seismic data recorded from four nuclear tests in the water-filled cavity in salt at Azgir, in which yield dependent cavity/tamped seismic source spectral ratios are estimated and interpreted in the context of theoretical simulations of the nonlinear interactions between the explosion-induced shock effects in both the water and surrounding salt medium. The report concludes with Section 4 in which a summary of the results of this research investigation is presented, together with some conclusions regarding the implications of these results to the evaluation of the cavity decoupling evasion scenario.

2
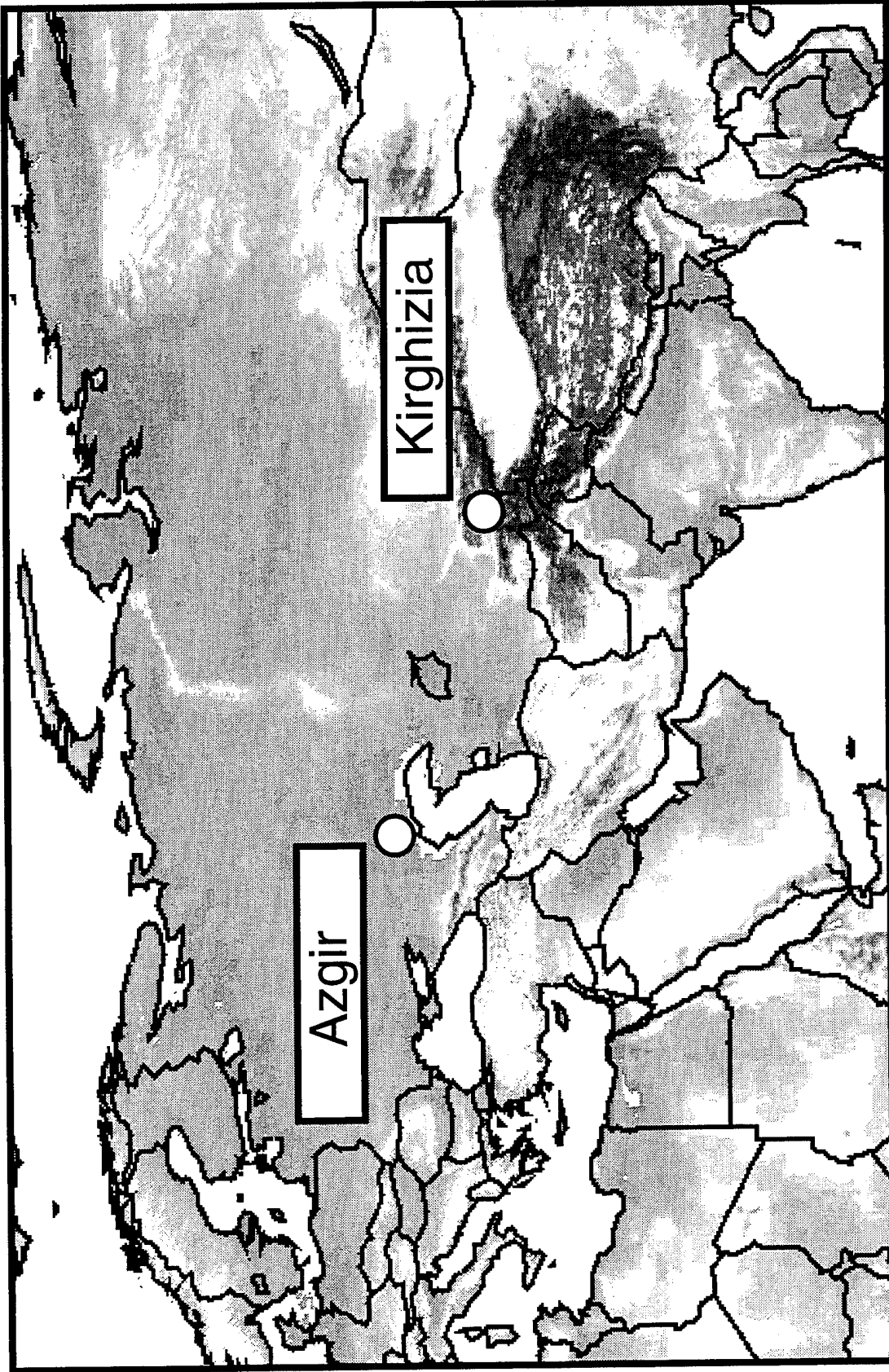
Figure 1. Map locations of the Azgir and Kirghizia cavity decoupling test locations.

2. KIRGHIZIA HE DECOUPLING TESTS

2.1 Overview

During the summer of 1960, the Russians carried out a series of HE cavity decoupling tests in limestone at a uranium mine in the Tywya Mountains of Kirghizia (40.4°N, 72.6°E). This test series was comparable in many ways to the COWBOY HE decoupling test series which was conducted in salt in the U.S. at about that same time (Herbst *et al.*, 1961), although it was somewhat more comprehensive in that it included a number of charge configurations which were not investigated in the COWBOY tests. In particular, the Kirghizia series included tests designed to evaluate the effects of cavity shape and charge emplacement geometry on decoupling effectiveness, in addition to conventional spherical cavity tests similar to those employed in COWBOY.

The emplacement conditions of these Kirghizia tests were described in detail in our previous report (Murphy *et al.*, 1994) and will only be briefly summarized here. The tests were conducted in chambers which were excavated off of the main mine access tunnel at a depth of about 290 m below the surface. Five decoupling chambers were excavated, including three spherical cavities with diameters in the 3.6 to 9.8 m range (i.e., radii of 1.81, 2.88 and 4.92 m), as well as two nonspherical chambers encompassing volumes of about 25 m^3, approximately equal to that of the 1.81 m radius spherical cavity. The shapes of these two nonspherical cavities were quite different. Chamber #6 was roughly cylindrical with a length (L) of about 6 m and height (H) and width (W) of about 2 m, giving an effective aspect ratio of about 3. Chamber #17, on the other hand, was considerably more elongated (L $\approx$ 12 m) and asymmetrical in cross-section (W = 2 m, H = 1 m), corresponding to an equivalent aspect ratio in the range of 6 to 12. Thus, data recorded from the tests in these chambers can provide a good measure of the dependence of decoupling effectiveness on cavity shape over a fairly wide range of cavity aspect ratios. These cavities were excavated in hard, homogeneous limestone, characterized by compressional wave velocities in the 5.5 to 6.0 km/sec range. The

4

maximum separation between any of the tests in the series was less than 150 m.

The test series was composed of 10 tamped and 12 decoupled explosions having yields of 0.1, 1.0 and 6.0 tons. The explosives consisted of ammonium nitrate, except for the two 6.0 ton tests which utilized a mix of TNT and ammonium nitrate. For the cavity tests, the explosives were suspended in the chambers and included cases in which the explosives were positioned in the center of the cavity, as well as cases in which they were positioned off-center, near the cavity walls. The configurations of the various cavity tests are graphically summarized for each of the five test chambers in Figure 2. It can be seen that explosions of the same yields were detonated in cavities of different size and also that explosions of different yields were detonated in two of the chambers (i.e. #10 and #13), thus providing redundant data which can be used to assess the effects of variations in scaled cavity size on decoupling effectiveness.

Before moving on to the analysis of the data, it is appropriate to consider how the yield/cavity volume ratios for these Kirghizia tests correspond to the common reference values of this ratio. Now, according to the simplified Latter criterion (Latter *et al.*, 1961) the volume of the cavity required to decouple an underground explosion is directly proportional to the yield of the explosion and inversely proportional to the overburden pressure at shot depth. It follows that the cavity radius required to decouple a nuclear explosion of yield W at a depth of 290 m in Kirghizia limestone to the same degree as that achieved for the 0.38 kt STERLING explosion in a 17 m radius cavity at a depth of 828 m in salt is given approximately as $32W^{1/3}$ m, for W in kilotons. Thus, the equivalent STERLING cavity radii for 0.1, 1.0 and 6.0 ton nuclear explosions at 290 m in limestone are about 1.5, 3.2 and 5.8 m, respectively. It follows that for HE/nuclear equivalence ratios in the range of 1 to 2, the 0.1 ton Kirghizia HE tests in the 1.81, 288 and 4.92 m radius cavities and the 1.0 ton test in the 4.92 m radius cavity should have been decoupled at least as effectively as STERLING, while the 1.0 ton test in the 2.88 m radius cavity and the 6.0 ton test in the 4.92 m radius cavity are somewhat overdriven with respect to STERLING, at least according to the Latter criterion.
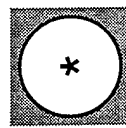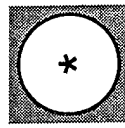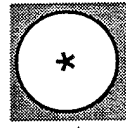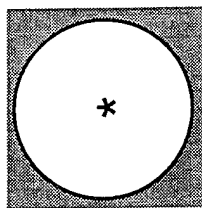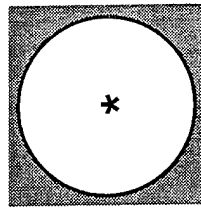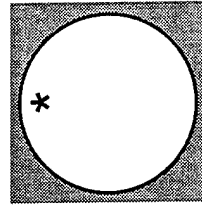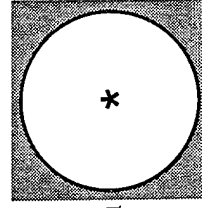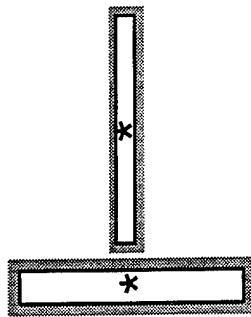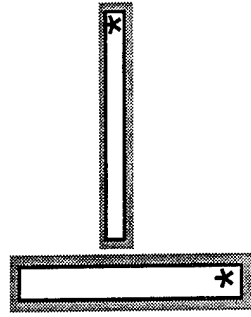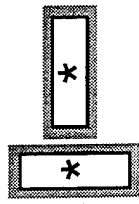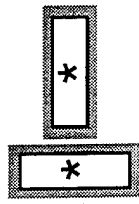
Figure 2. Graphical summary of the HE decoupling tests conducted in each of the excavated explosion chambers. The asterisk denotes the emplacement location of the charge within the chamber for each test. For the nonspherical cases, both horizontal (left) and vertical (right) sections through the chambers are displayed.

6

These highly simplified calculations provide a rough basis for evaluating the Kirghizia limestone data in terms of previous experience in salt.

Seismic data were recorded from these Kirghizia tests at locations in the mine over a distance range extending from about 10 to 250 m from the sources (Kitov et al., 1995). Most of these data were recorded on broadband velocity (VIB) sensors which were installed in drill holes and niches excavated in the wall of the mine. Peak amplitudes of displacement and velocity have been reported for over 250 of these recording locations and these peak data are analyzed and compared in the following section. Waveform data were recovered for only about 30 of these recordings and these were digitized at IDG and form the basis for the frequency dependent decoupling analysis presented in Section 2.3.

2.2 Analysis of the Peak Amplitude Data

Some preliminary analyses of the Kirghizia peak amplitude data were presented in our previous report (Murphy et al., 1994) and, more recently, Kitov et al. (1995) have performed statistical analyses of the complete data set on a test by test basis. Kitov et al. (1995) concluded from the results of these statistical analyses that there are some systematic differences in amplitude levels and distance attenuation rates between tests which may correlate with yield and scaled cavity size. While these results may provide some important new constraints on the equation of state to be used in theoretical simulations of explosions in limestone, the inferred differences between tests are fairly subtle with respect to the scatter in the data and do not affect the principal decoupling issues being addressed in this study. Therefore, in the following analyses we will rely primarily on direct comparisons of the low frequency peak displacement data observed from the various tests, rather than on these statistical fits to the data.

As an initial example, Figure 3 shows a comparison of the peak displacement data as a function of range observed from a 1.0 ton tamped shot and the 1.0 ton decoupled test in the 2.88 m radius spherical cavity. It can be seen from this figure that the cavity test was indeed decoupled in

7
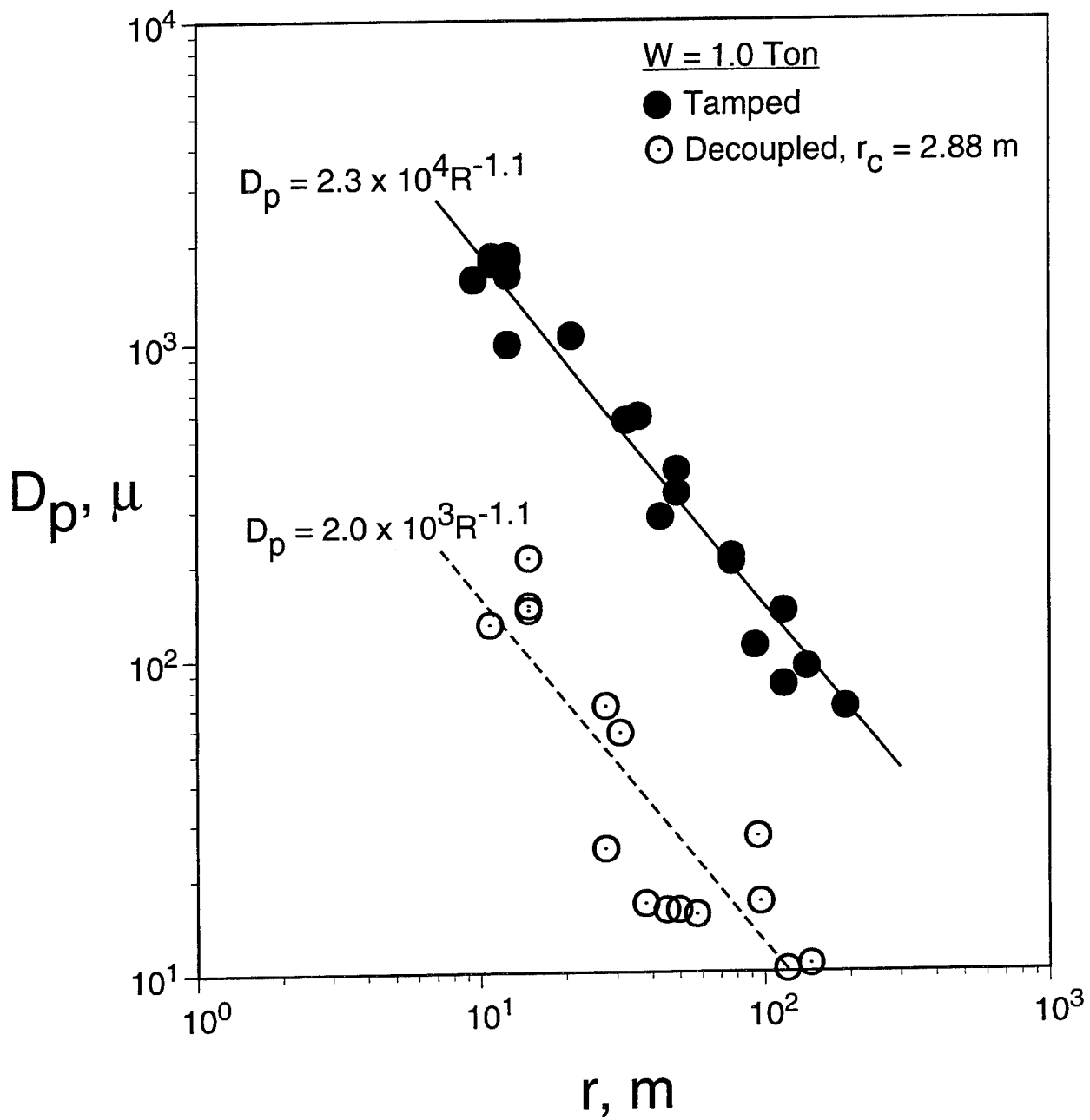
Figure 3. Comparison of peak displacement data as a function of range observed from 1.0 ton tamped and cavity decoupled HE tests at Kirghizia.

this case, showing an average peak displacement decoupling factor of about a factor of ten with respect to the tamped shot of the same yield. Note that this value is significantly lower than the nominal low frequency decoupling factor of about 70 which is generally associated with the fully-decoupled tests of the U.S. STERLING and COWBOY series. However, it is important to note that the peak displacements being compared in Figure 3 correspond to very different frequency components and therefore, can not be directly interpreted in terms of the low frequency decoupling level which is typically used to quantify decoupling efficiency. This fact is clearly illustrated in Figure 4 which shows a comparison of the radial particle velocity seismograms recorded at a range of about 100 m from these two explosions. Note that these data are consistent with the theoretically expected differences in dominant frequency content between tamped and cavity decoupled explosions of the same yield. That is, because the characteristic seismic source radius is considerably larger for a tamped explosion than for a cavity decoupled explosion of the same yield, the characteristic corner frequency of the tamped seismic source is expected to be lower, as observed in Figure 4. It follows that spectral analyses of such complete waveform data are required in order to accurately estimate the absolute levels of the low frequency decoupling factors for these tests.

However, despite the fact that peak amplitude data are not well-suited for establishing absolute levels of decoupling effectiveness, they do provide a reasonable basis of comparison which can be used to assess the relative effects of variables such as yield, cavity size and shape and charge emplacement geometry. That is, while the dominant frequencies of the peak motions corresponding to tamped and cavity decoupled explosions of the same yield are observed to be quite different, those associated with decoupled explosions of the same yield in different cavities are observed to be very similar. This fact is illustrated in Figure 5 which shows the particle velocity seismograms recorded at a range of about 100 m from 1.0 ton decoupled explosions in cavities with radii of 2.88 and 4.92 m. It follows that peak amplitude readings obtained from such recordings can be directly compared to estimate differences in decoupling effectiveness at a common dominant frequency. For example, Figure 6 shows a comparison of the peak displacement data as a function of range observed from 0.1 ton

9

Tamped 1.0 ton

Decoupled 1.0 ton
$r_c = 2.88m$

.01 sec
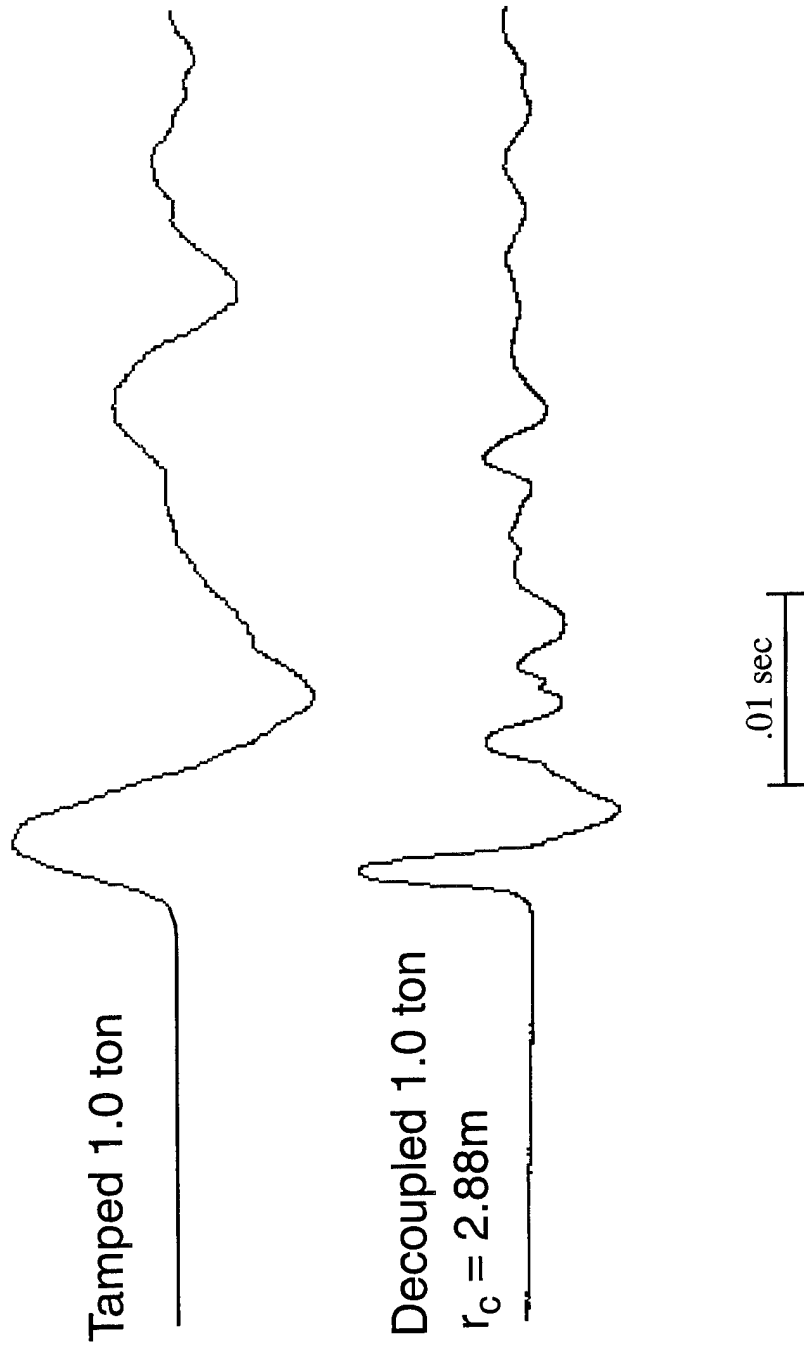
Figure 4. Comparison of radial particle velocity seismograms recorded at a range of about 100m from 1.0 ton tamped and cavity decoupled Kirghizia explosions.
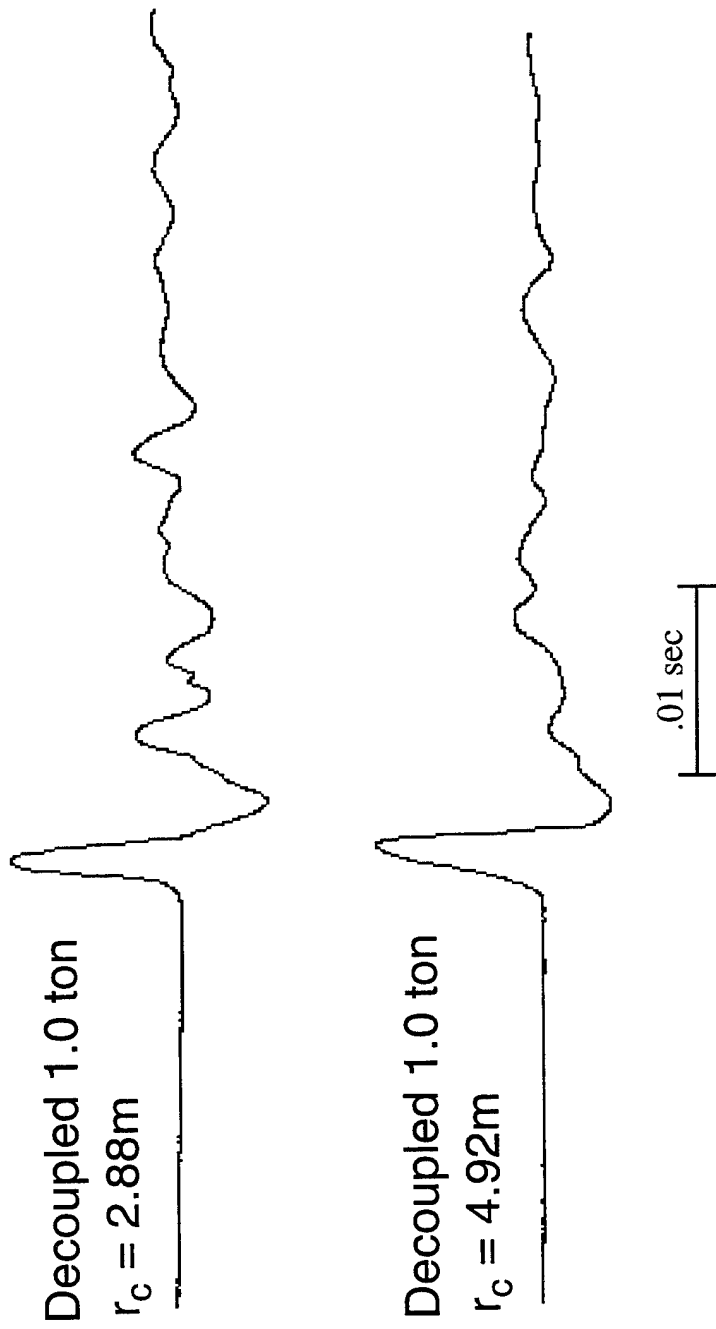
Figure 5. Comparison of radial particle velocity seismograms recorded at a range of about 100m from 1.0 ton cavity decoupled Kirghizia explosions in cavities with radii of 2.88 and 4.92m.
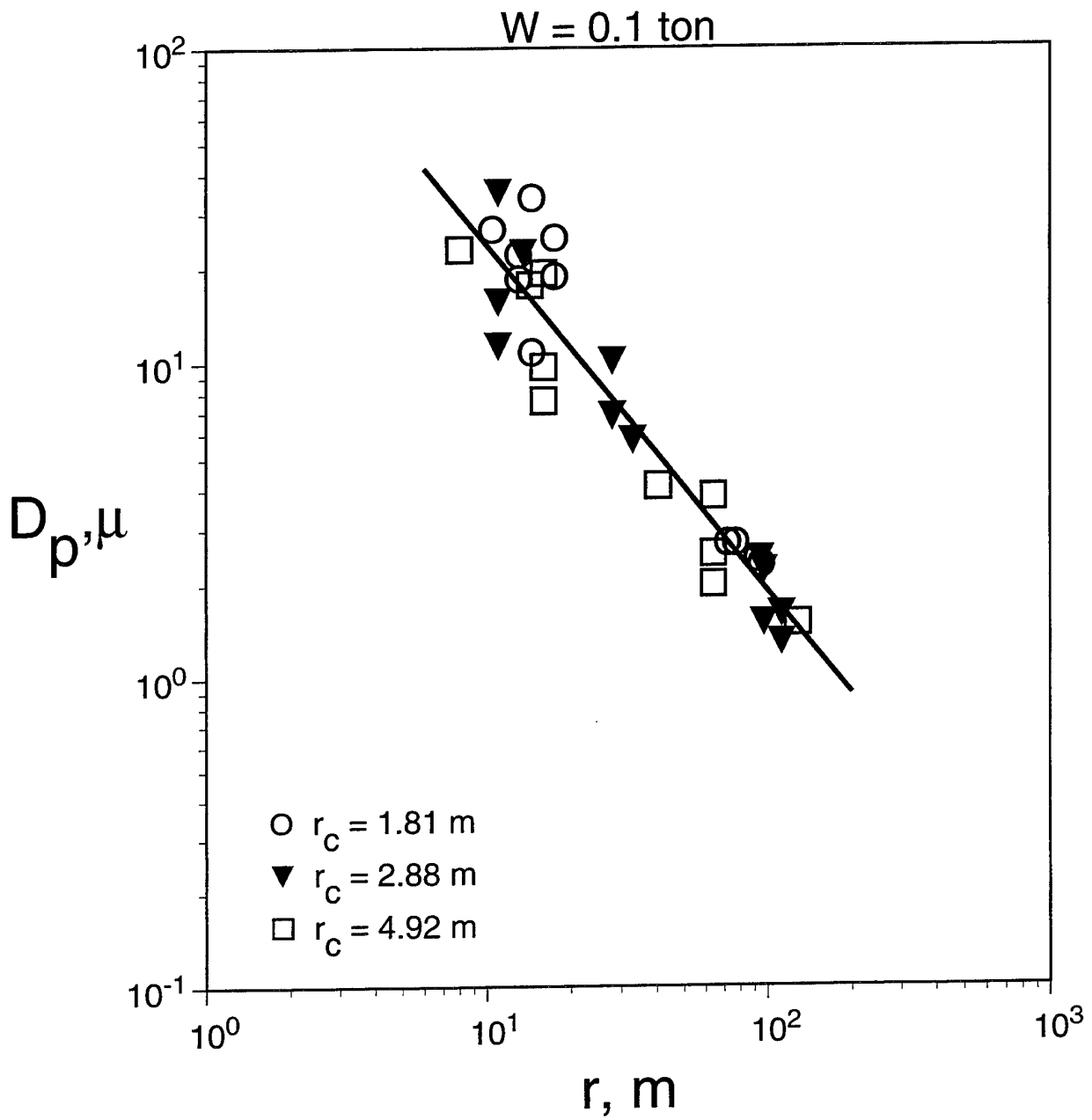
Figure 6. Comparison of peak displacement data as a function of range observed from 0.1 ton decoupled tests in spherical cavities with radii of 1.81, 2.88 and 4.92m.

decoupled tests in the spherical cavities with radii of 1.81, 2.88 and 4.92 m. Now, according to elementary theory, once the cavity is large enough to fully decouple an explosion of a given yield, the low frequency level of the seismic source function is expected to be independent of cavity radius for any larger cavities (Murphy, 1980). That is, in the low frequency limit, the seismic source level corresponding to the linear, elastic response of the cavity wall to a late-time, steady-state pressure P in the cavity is proportional to Pr_c^3 and, since P is inversely proportional to cavity volume, this source level is independent of cavity radius once the linear, elastic limit has been reached. It can be seen from Figure 6 that the observed peak displacement levels for these three 0.1 ton tests appear to be independent of cavity radius over this range, which suggests that essentially full decoupling was achieved in all three of these tests. This is not surprising in that, as was noted previously, all three of these cavities are larger than that of STERLING scaled to this yield and overburden pressure. It does, however, serve to confirm the fact that such low frequency peak displacement data are useful for comparing the relative seismic efficiency of different decoupling tests.

A similar comparison for the 1.0 ton decoupled tests in the centers of spherical cavities with radii of 2.88 and 4.92 m is presented in Figure 7. In this case, the 2.88 m radius cavity is predicted to be overdriven somewhat with respect to STERLING, while the 4.92 m radius cavity test is expected to be fully decoupled. However, once again the observed peak displacement levels from the two tests appear to be quite comparable, suggesting that both tests were essentially fully decoupled.

Another way of comparing these same data is to look at scaled peak displacements for explosions of different yields in the same cavity. That is, by the same simple, elastic theory referenced above, the low frequency level of the seismic source function is expected to be directly proportional to yield for cavities large enough to fully decouple the explosions. Therefore, to the extent that the observed peak displacement data are proportional to the low frequency levels of the corresponding seismic source functions, they should scale as the first power of the yield for fully decoupled explosions in a given cavity. The results of applying this model

13
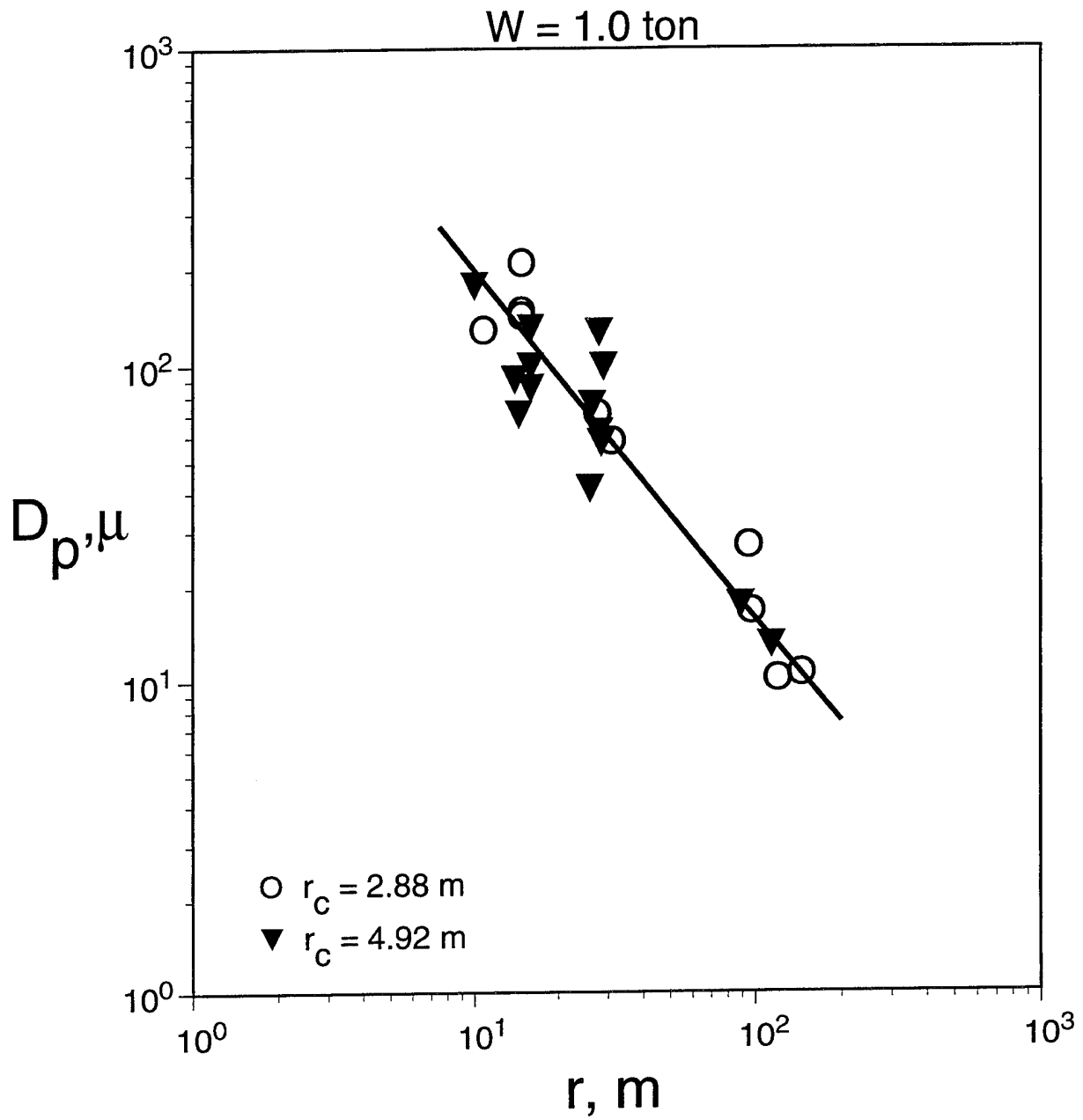
Figure 7. Comparison of peak displacement data as a function of range observed from 1.0 ton decoupled tests in spherical cavities with radii of 2.88 and 4.92m.

to the tests in the 2.88 m radius spherical cavity are presented in Figure 8, where the yield scaled peak displacements as a function of range observed from the 0.1 and 1.0 ton explosions in that cavity are compared. It can be seen that these yield scaled peak displacement values are very consistent, which provides further evidence that the 1.0 ton explosion in this cavity was essentially fully decoupled. Figure 9 shows a similar comparison of yield scaled peak displacements as a function of range for the 0.1, 1.0 and 6.0 ton decoupled tests in the center of the 4.92 m radius spherical cavity. Here again, the yield scaled peak displacement levels are found to be in excellent agreement, indicating that all three of these tests were fully decoupled. We conclude that the available peak amplitude evidence indicates that all the tests detonated in the center of these three spherical cavities were essentially fully decoupled. These results are summarized in Figure 10 which shows the yield scaled peak displacement levels for the different cavity tests, plotted as a function of scaled cavity radius ($r_c/W^{1/3}$). For the purposes of this comparison, the relative peak displacement levels were estimated by computing least-squares amplitude/distance relations for each test, assuming a nominal attenuation rate of $r^{-1.1}$(Murphy et $al.$, 1994), corresponding to the slope of the straight lines on Figures 6-9. It can be seen from Figure 10 that these yield scaled peak displacement levels show no obvious trend as a function of scaled cavity radius over the range extending from 27 to 106 $m/kt^{1/3}$. The average scaled (i.e., W = 1 ton, r = 1 m) peak displacement level for these cavity tests is 2800μ, with a total range of only about ± 25% around this mean value. We conclude that HE tests in spherical cavities with radii larger than 27 $m/kt^{1/3}$ under this overburden pressure in Kirghizia limestone are essentially fully decoupled.

The effects of charge emplacement geometry are addressed in Figure 11, which shows a comparison of the peak displacement data as a function of range observed from the two 1.0 ton tests conducted at different locations in the 4.92 m radius spherical cavity. In this case, one test was conducted with the charge positioned in the center of the cavity, while the other was conducted with the charge centered 1 m from the cavity wall. It can be seen from this figure that the observed peak displacement level for the test near the cavity wall appears to be somewhat larger on average than that observed from the corresponding test in the center of the cavity. This
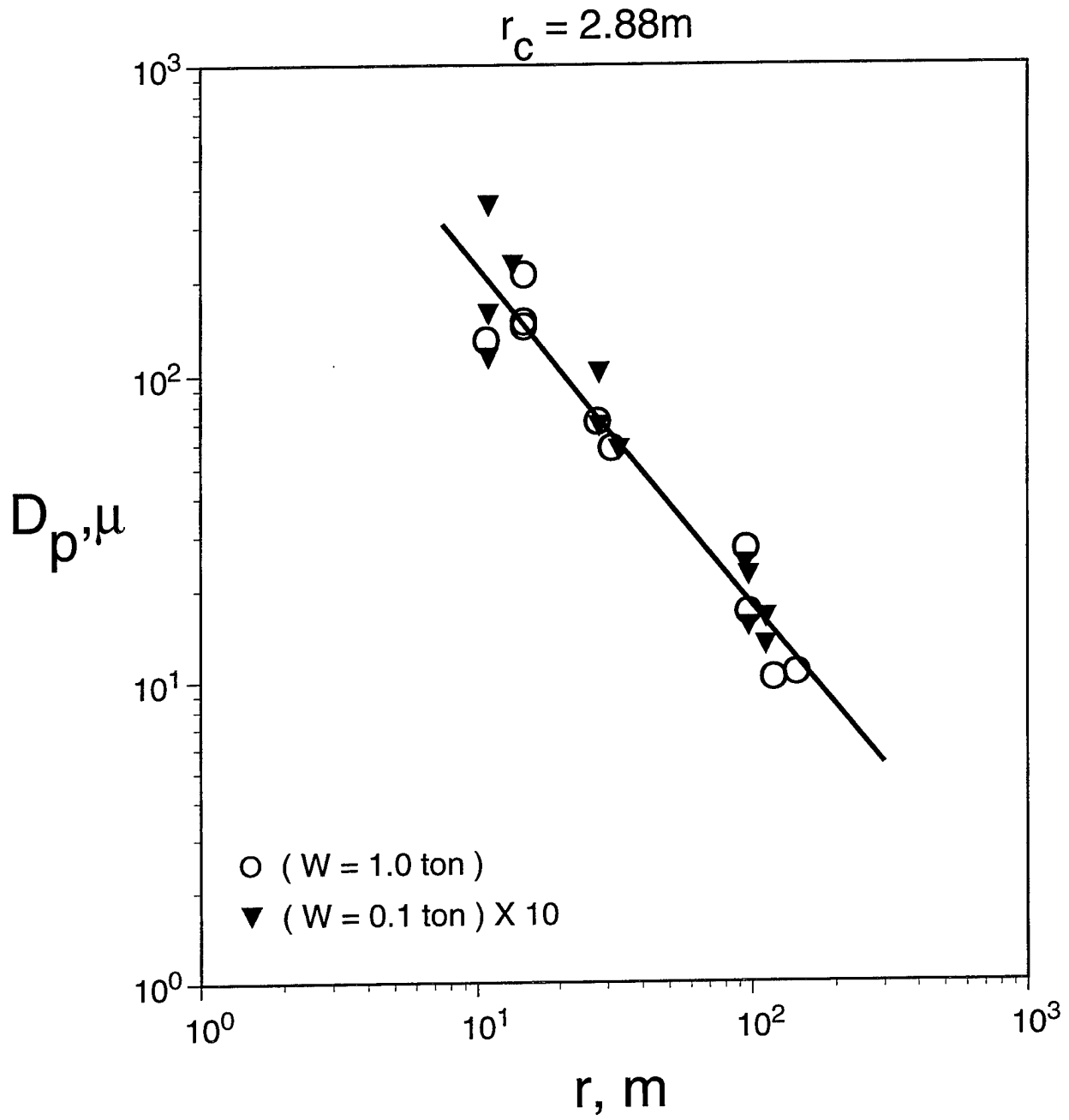
Figure 8. Comparison of yield scaled peak displacement data as a function of range for 0.1 and 1.0 ton decoupled tests in the spherical cavity with radius 2.88m.
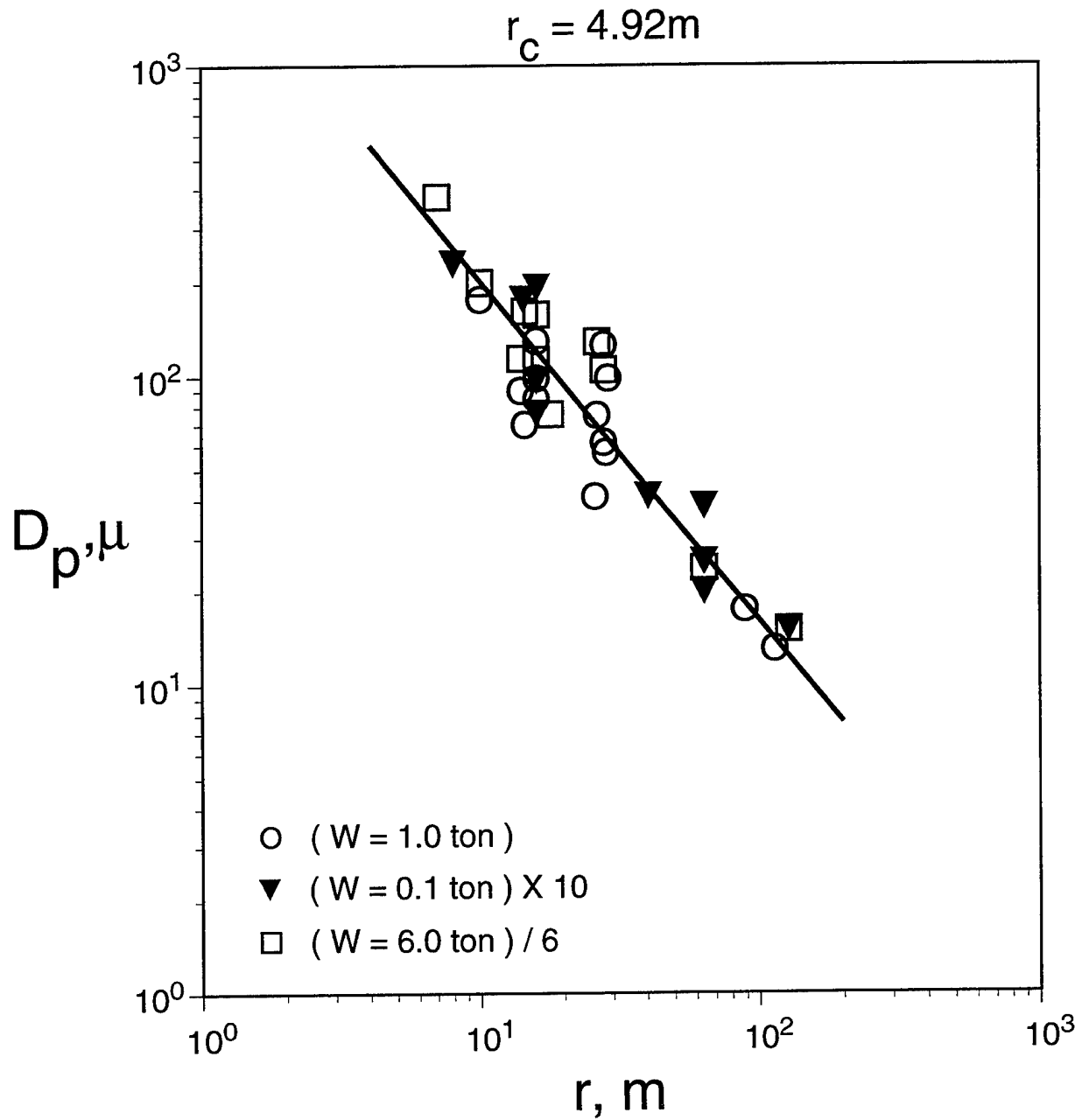
Figure 9. Comparison of yield scaled peak displacement data as a function of range for 0.1, 1.0 and 6.0 ton decoupled tests in the spherical cavity with radius 4.92m.

17
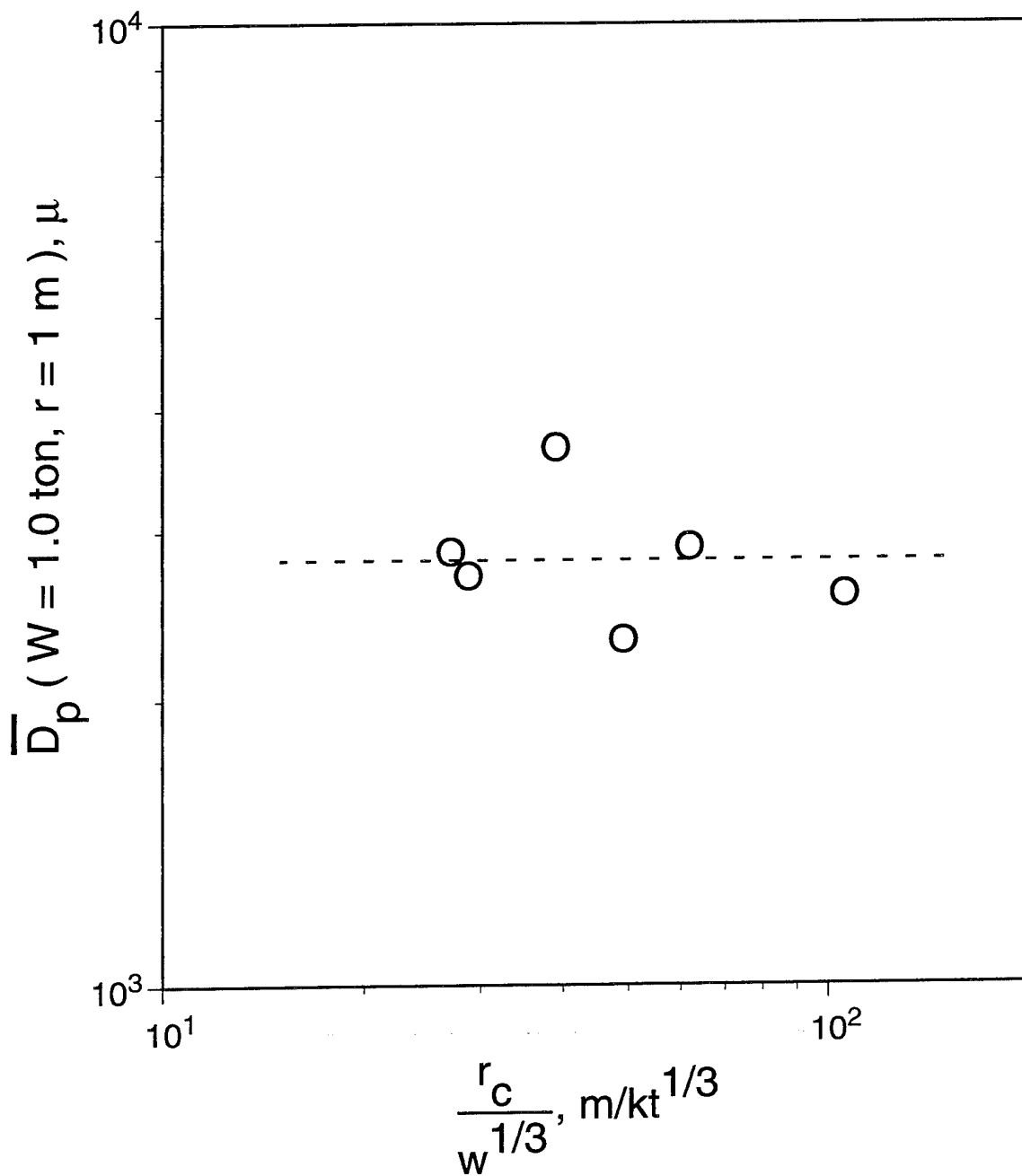
Figure 10. Comparison of yield scaled peak displacement levels as a function of scaled cavity radius for Kirghizia decoupled HE tests in the center of spherical cavities at a depth of 290m in limestone.

18
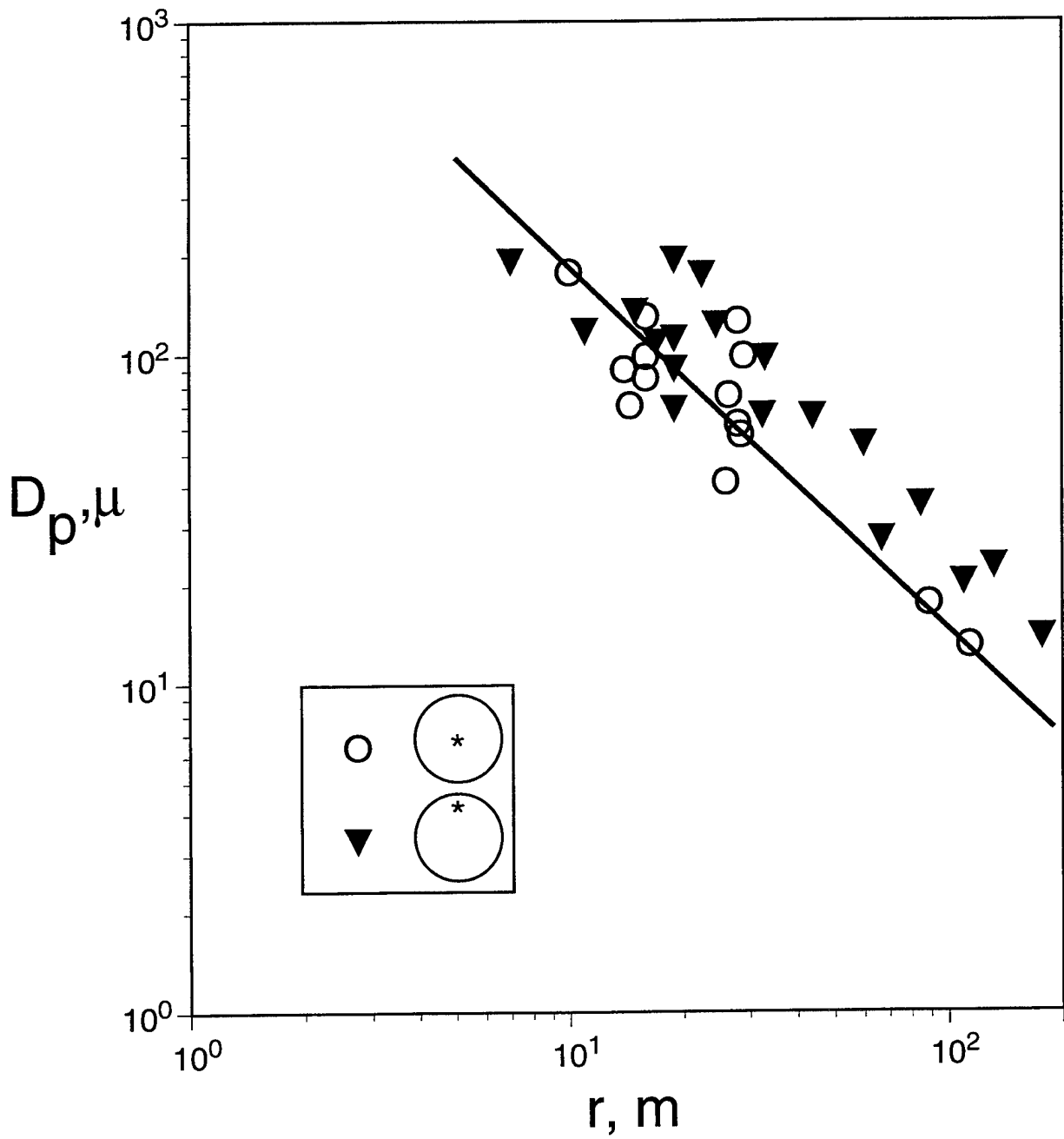
Figure 11. Comparison of peak displacement data observed from 1.0 ton decoupled tests at different locations in the 4.92m radius spherical cavity.

suggests that the proximity of the charge to the cavity wall in the former test resulted in an increase in the degree of nonlinear response in the surrounding medium and, hence, increased seismic coupling efficiency in that case. That is, the decoupling efficiency has been somewhat reduced as a result of this charge emplacement geometry. However, the magnitude of this effect appears to be no more than a factor of two in this case, at least in the frequency range represented by this peak displacement data.

As was noted previously, in addition to the spherical cavity decoupling tests described above, the Kirghizia series included several tests designed to assess the influence of cavity shape on decoupling effectiveness. This is a very important practical issue in that, from an engineering perspective, it is much easier to construct elongated, tunnel-like cavities than it is to construct underground spherical cavities of the same volume. A number of theoretical studies of this problem have been conducted in recent years (Steven et al., 1991b; Rimer et al., 1994) and the results of these studies have indicated that the low frequency decoupling effectiveness is largely independent of cavity shape, even for elongated cavities with aspect ratios of 10 to 1 or more. However, until now, no experimental data have been available to test these theoretical simulation results. Figure 12 shows comparisons of the peak displacement versus range data observed from the Kirghizia 0.1 ton decoupled tests in spherical and cylindrical cavities of about the same volume (i.e., 25 m^3). The left and center panels in this figure show comparisons for the explosions detonated in the center of test chambers #6 and #17 (Cf. Figure 2), respectively. It can be seen from these plots that the peak displacement levels observed from these two tests in elongated cavities are very comparable to those observed from the test in the spherical cavity of the same volume over the entire distance range of observation. These results provide strong evidence that the low frequency decoupling effectiveness is approximately independent of cavity shape for elongated cavities with aspect ratios of 6 or more. The right hand panel in Figure 12 shows a similar comparison for the test detonated 1 m from the end of chamber #17. In this case, the closest observations at ranges less than about 10 m show evidence of some enhanced coupling relative to the corresponding spherical cavity observations, but once again these differences appear to be less than a factor of 2. Moreover, although
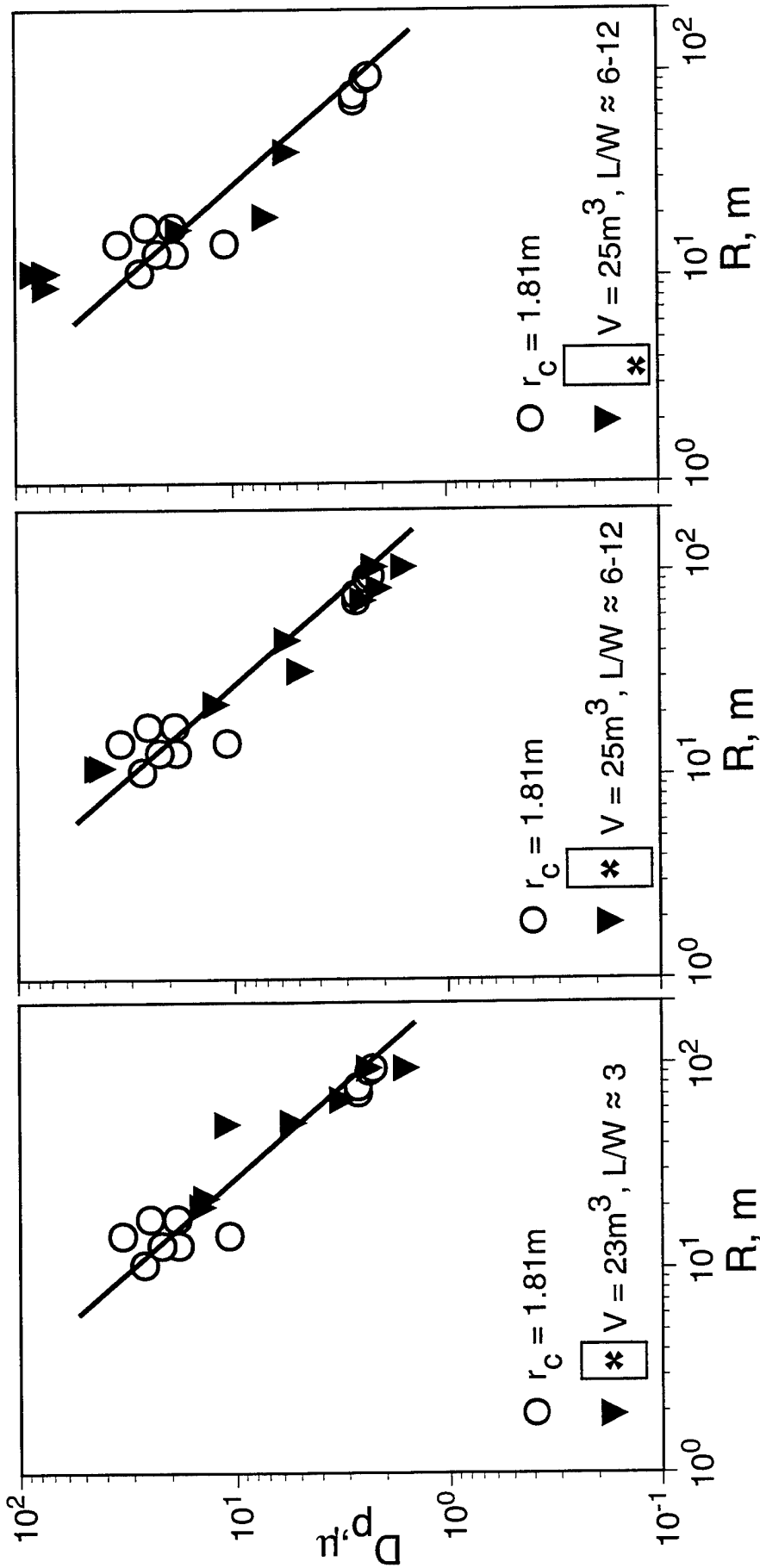
Figure 12. Comparison of peak displacement data observed from Kirghizia 0.1 ton decoupled tests in spherical and elongated cavities of comparable volume. For the nonspherical cavities, the asterisks denote the charge location.

the data are sparse, even these relatively small differences seem to disappear at observation distances greater than the long dimension of the cavity. This is a somewhat surprising result given the corresponding spherical cavity observations of Figure 11, and suggests that this charge emplacement geometry issue deserves additional study. In any case, we conclude that over the range of test conditions explored at Kirghizia, the low frequency decoupling effectiveness depends only on cavity volume and is roughly independent of the shape of the cavity, in agreement with our previous theoretical simulation results (Stevens *et al.*, 1991b; Rimer *et al.*, 1994).

2.3 Analysis of the Waveform Data

It was noted above that the waveform data which are currently available from the Kirghizia decoupling test series are much less complete than the peak motion data. In particular, of the more than 250 recordings from which peak motion values were determined, waveform data were recovered from only about 30, all of which have now been digitized at IDG and previewed for possible spectral analyses. Unfortunately, more than half of these waveforms were found to be complete only through the first half cycle of motion and these proved to be of limited value for quantitative evaluation of the frequency dependent decoupling on these tests. Moreover, of the remaining complete waveforms, a number were recorded from 0.1 ton tamped tests for which there were no corresponding recordings from cavity decoupled tests of the same yield. Thus, the only waveform data which proved to be useful for quantitative spectral analyses were the few recorded from 1.0 ton tamped and decoupled tests in the 2.88 m and 4.92 m radius spherical cavities. The radial component particle velocity seismograms recorded in the distance range of 77 to 193 m from two different tamped 1.0 ton Kirghizia tests are plotted in Figure 13, while the corresponding seismograms recorded from two 1.0 ton cavity decoupled tests are reproduced in Figure 14. The top trace in Figure 14 was recorded from the 1.0 ton explosion in the center of the 2.88 m radius cavity, while the bottom two traces in this figure were recorded from the 1.0 ton explosion detonated 1 m from the wall of the 4.92 m radius cavity.

22
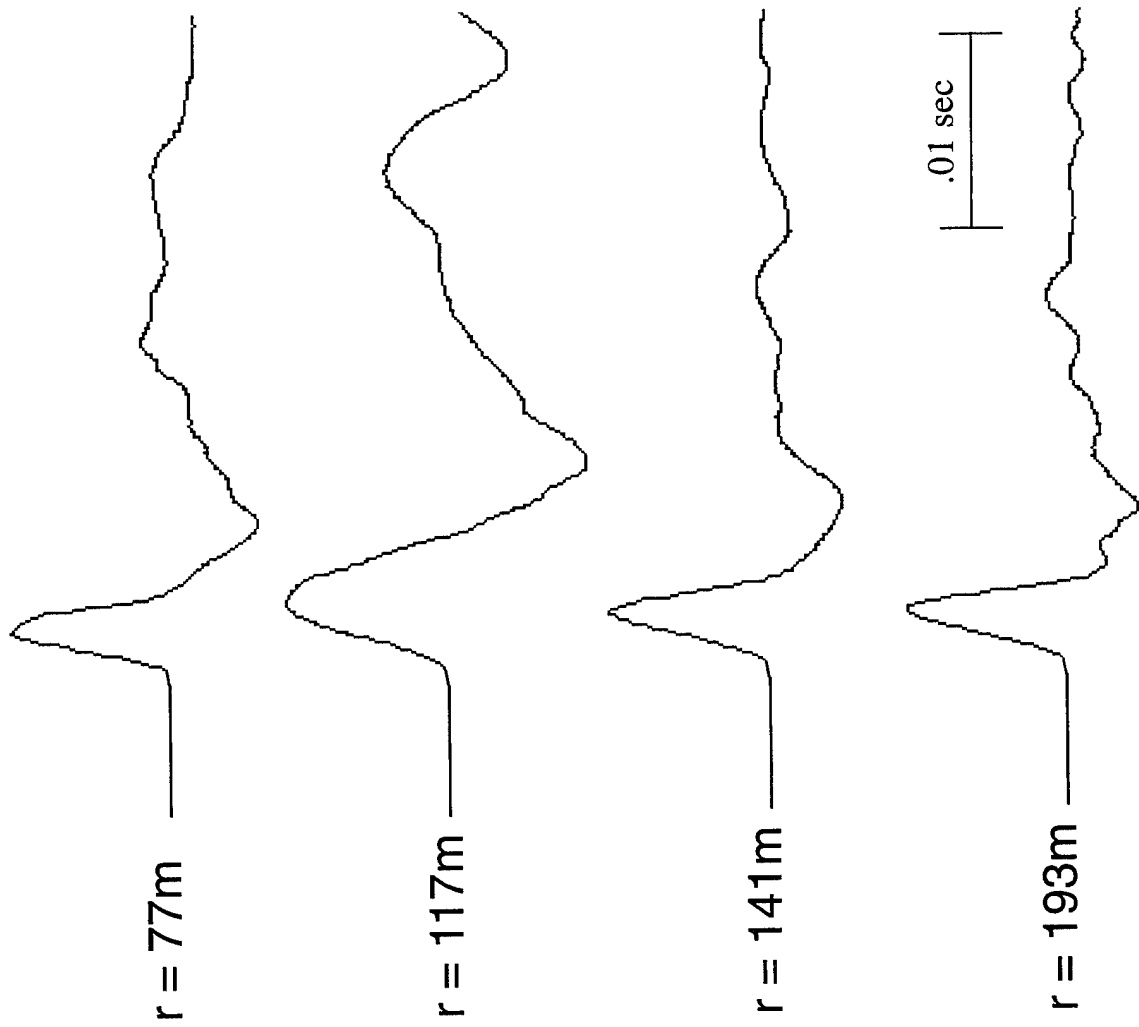
Figure 13. Radial component particle velocity seismograms recorded from 1.0 ton tamped Kirghizia explosions.

r = 77m

r = 117m

r = 141m

r = 193m

.01 sec
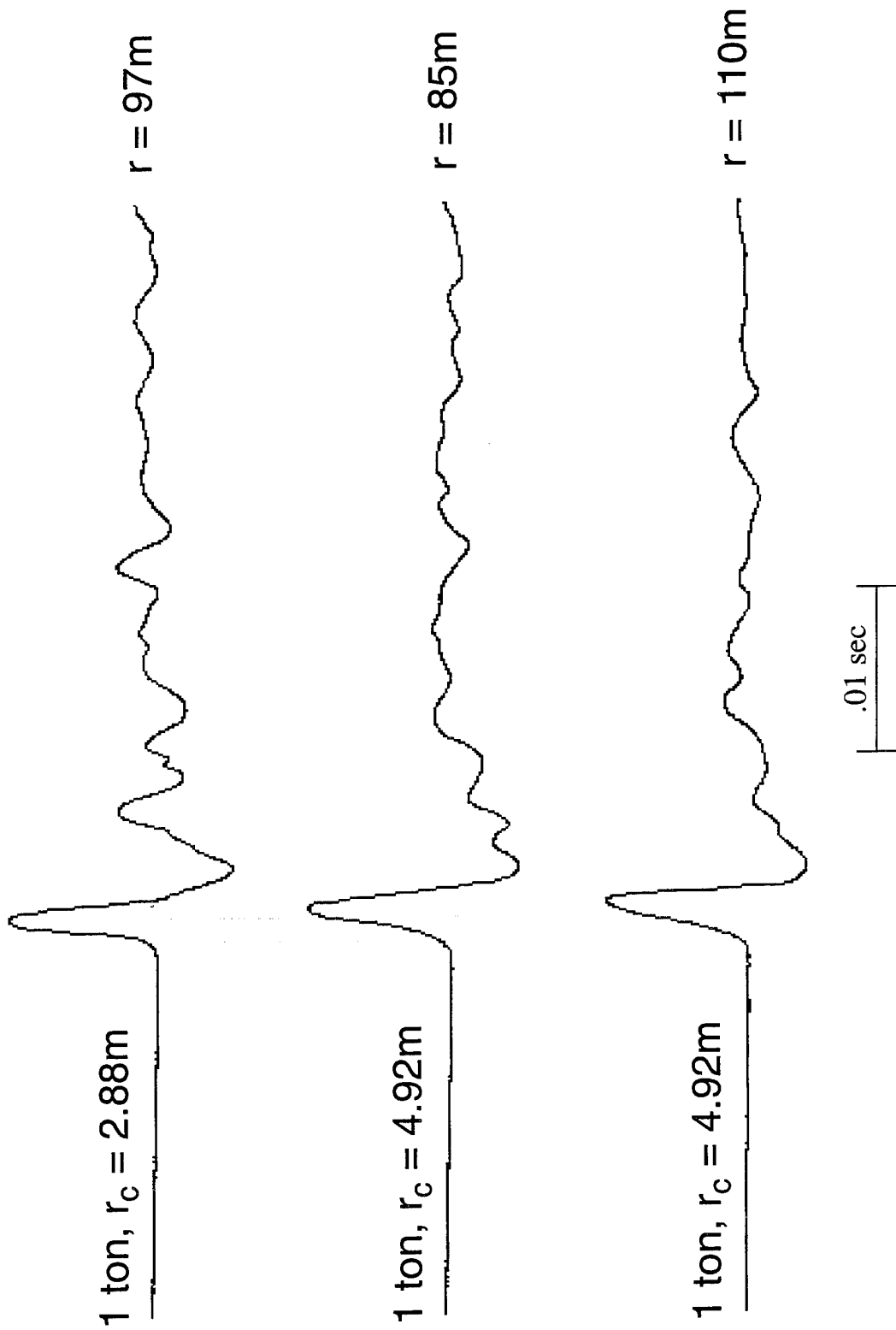
Figure 14. Radial component particle velocity seismograms recorded from 1.0 ton decoupled Kirghizia explosions in the center of a 2.88m radius spherical cavity (top) and 1.0 meter from the wall of a 4.92m radius spherical cavity (center and bottom).

It can be seen that these three decoupled test waveforms were all recorded at a range of about 100 m, a distance which is encompassed by the ranges of the four tamped recordings of Figure 13.

Although detailed analyses of the spectra corresponding to the tamped waveforms of Figure 13 revealed that the amplitude attenuation with distance in the Kirghizia limestone is frequency dependent, as would be expected, the decoupling analysis results were found to be insensitive to the details of this frequency dependence, because the available recorded data sample such a limited distance range. Consequently, Kitov *et al.* (1995) proceeded by normalizing all the data to a reference distance of 110 m using the nominal, frequency independent peak velocity attenuation law $r^{-1.75}$. Following this distance normalization, tamped to decoupled spectral ratios were computed using each of the four tamped recordings and the results were then averaged to estimate the decoupling factors as a function of frequency. The result for the 1.0 ton explosion in the center of the 2.88 m radius cavity is shown in Figure 15, where it can be seen that the maximum low frequency decoupling at the corner frequency of the tamped shot (i.e., around 75 Hz) is about a factor of 25 for this HE test. This value is significantly lower than the preliminary estimate of 50 cited in our previous report (Murphy *et al.*, 1994) and reflects the correction of an erroneous data calibration factor used in that analysis. The dotted lines in Figure 15 denote the 95% confidence interval around the mean spectral ratio, and it can be seen from these bounds that the frequency dependent decoupling estimates obtained using the four different tamped recordings are quite consistent, particularly at low frequencies. This measure of uncertainty is limited, of course, by the fact that only one recording is available from the decoupled test. Thus, the accuracy of the decoupling estimate is critically dependent on the assumption that this one recording is representative of that test. In the absence of additional data, about all that can be said in this regard is that the peak displacement value corresponding to this recording is indeed close to the expected mean value for that test (Cf. Figure 7).

The observed maximum low frequency decoupling factor of 25 for this presumably fully decoupled Kirghizia test is considerably lower than
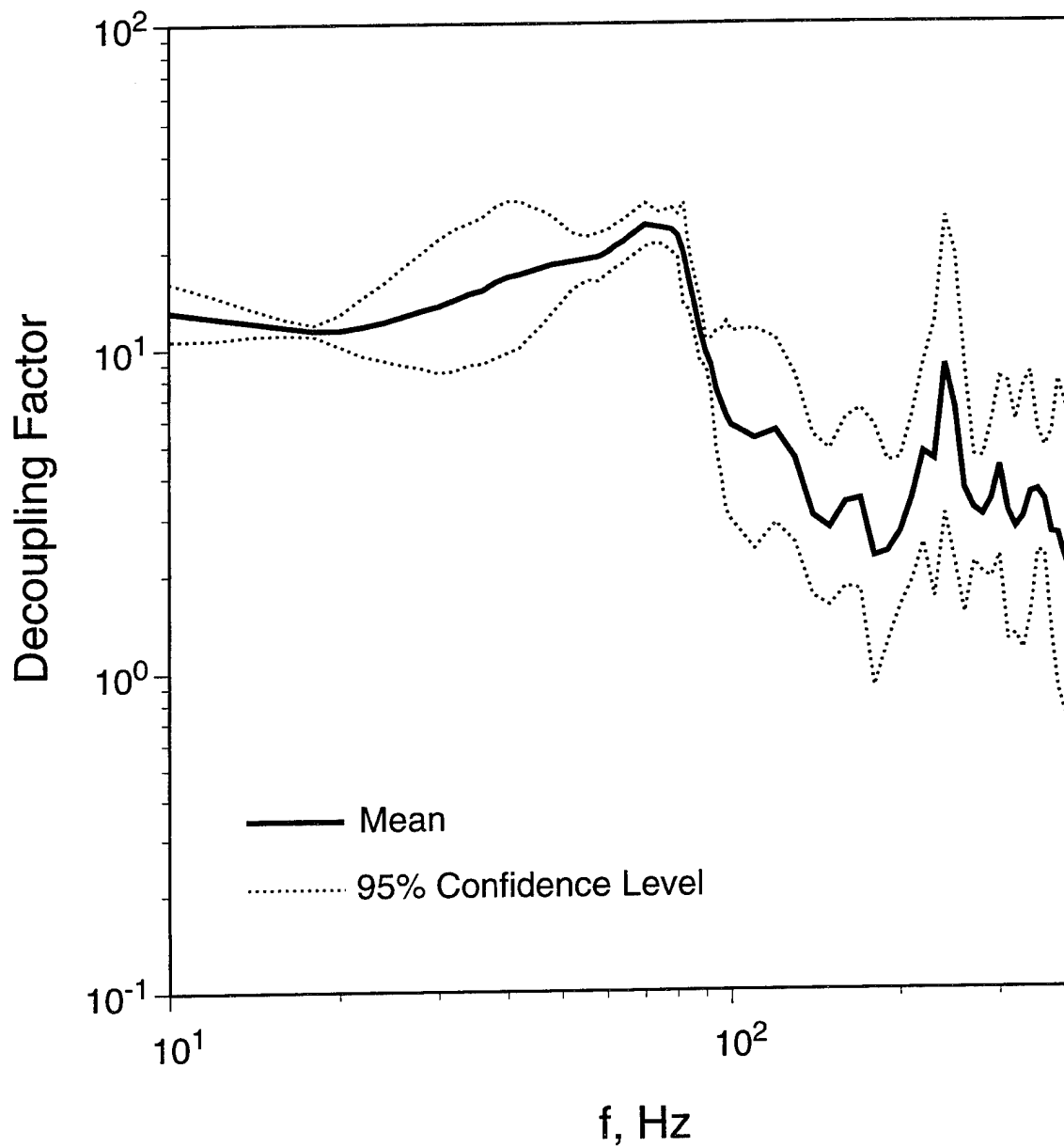
Figure 15. Frequency dependent decoupling factor corresponding to a 1.0 ton
Kirghizia explosion in the center of a 2.88m radius spherical cavity.

the nominal full decoupling factor of 70 which is usually quoted on the basis of STERLING experience. Although a number of recent theoretical simulation studies have indicated that, for a given cavity size, HE explosions are expected to decouple less effectively than nuclear explosions of the same yield in salt (Glenn and Goldstein, 1994; Murphy *et al.*, 1996), the observed decoupling factors for the fully decoupled COWBOY HE tests appear to have been about 70 (Murphy, 1980), close to that reported for STERLING. However, very little decoupling data have been reported from tests in media other than salt. Reinke *et al.* (1995) have recently described some preliminary results obtained from the analysis of data recorded from cavity decoupled HE tests conducted in limestone in a mine near Magdalena, New Mexico. In these tests, explosions with a wide range of yields (i.e., 0.1 to 4.0 tons) were detonated in rectangular chambers of fixed dimensions (i.e., 2m x 4m x 8.5 m). These tests were somewhat limited, however, in that these chambers were not sealed and the explosive pressures were vented to the main mine adit via a narrow access passageway to the chamber. Thus, the applicability of these decoupling data is subject to some uncertainty, particularly at the low frequencies of primary interest. In any case, Reinke *et al.* (1995) report low frequency decoupling factors for the Magdalena tests which range from about 10 to 70 for those cavity tests with scaled yield/volume ratios comparable to that of the 1.0 ton Kirghizia test in the 2.88 m radius spherical cavity. Thus, these two limestone HE decoupling estimates are consistent within the rather large data scatter.

A spectral analysis similar to that described above for the 2.88 m radius cavity test was also conducted using the two waveforms from Figure 14 which were recorded from the 1.0 ton decoupled test detonated near the wall of the 4.92 m radius cavity. The resulting average frequency dependent decoupling factor for this test is shown as a dashed line in Figure 16, where it is compared with the corresponding average decoupling factor from Figure 15. It can be seen that the maximum observed low frequency decoupling for this test is about a factor of 10, which is 2.5 times lower than that observed for the 1.0 ton decoupled test in the center of the 2.88 m radius cavity. That is, these spectral data are generally consistent with the peak displacement data of Figure 11, which were interpreted to indicate
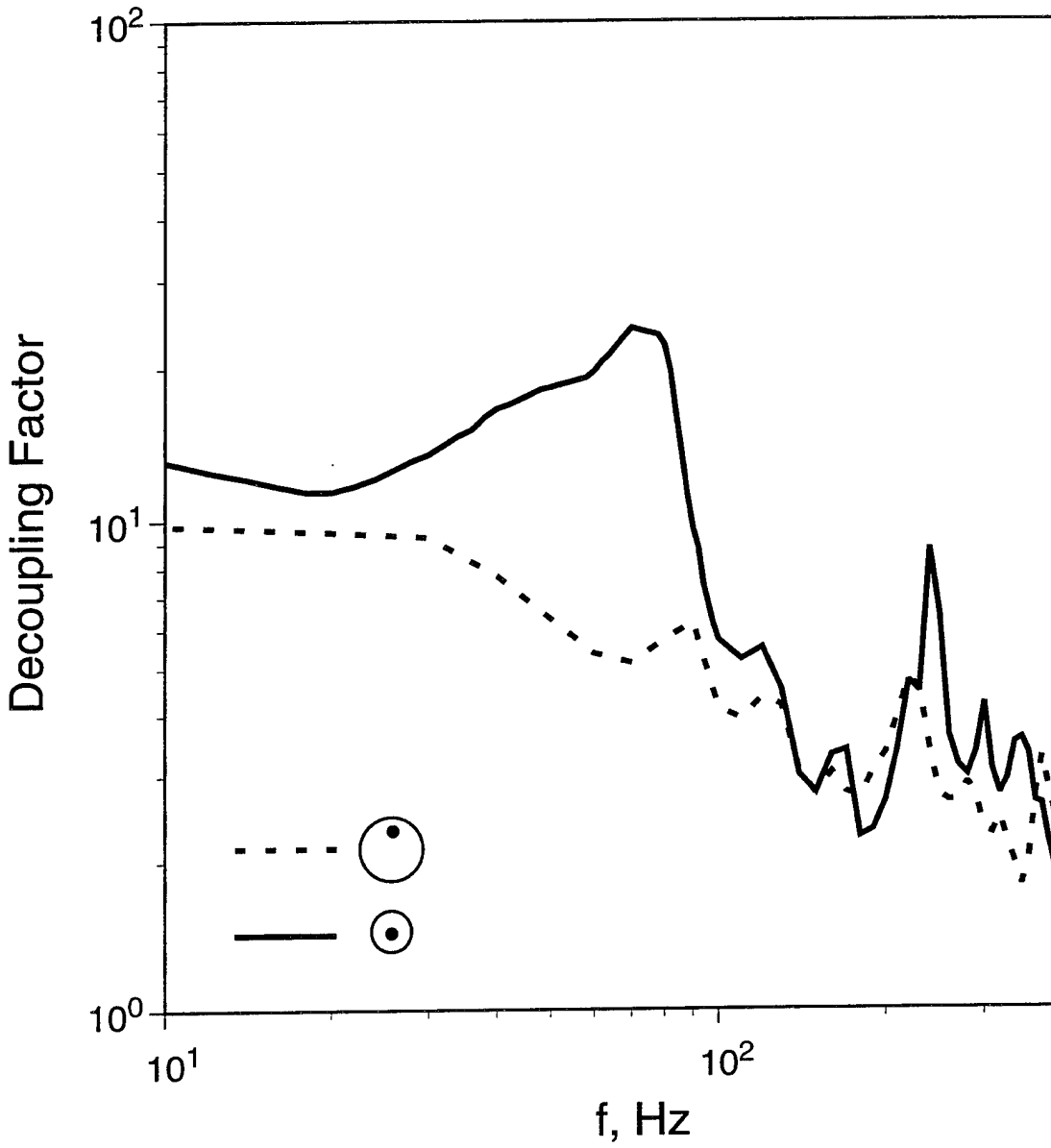
Figure 16. Comparison of frequency dependent decoupling factors determined for 1 ton Kirghizia explosions in the center of a 2.88 m radius spherical cavity (solid) and near the wall of a 4.92 m radius spherical cavity (dashed).

28

that proximity to the cavity wall had increased the low frequency seismic coupling efficiency by about this amount for that test. Note also from Figure 16 that this difference in decoupling effectiveness is frequency dependent and that it reaches a maximum of more than a factor of 4 at around 80 Hz, where the decoupling is maximum for the 2.88 m radius cavity test. Thus, the effects of charge emplacement geometry appear to be complex, and additional theoretical simulation studies and experimental tests will be required in order to define these effects in a quantitative fashion.

2.4 Theoretical Simulation Analysis

In order to carry out theoretical simulations of explosions in a particular medium, it is first necessary to specify an equation of state for the geologic material which applies over the entire range of pressures induced by the explosive sources. Such information is presently not available for the Kirghizia limestone medium and, consequently, it has been necessary to approximate the required equation of state using data on limestone from other locations. The only site specific material properties reported by Kitov *et al.* (1995) for the Kirghizia limestone were the density and compressional wave velocity. Therefore, these values were combined with reported data from other limestones to establish the nominal set of elastic constants listed in Table 1, which have been adopted for simulation purposes.

The volumetric equation of state used in the calculations was calibrated to match the Hugoniot data for limestone given by Schuster *et al.* (1991) in the pressure range from 10 - 200 kb. The polynomial fit to this Hugoniot is given by

$$P = K \mu + B (\mu - \mu_0)^2 \qquad \text{for } \mu > \mu_0$$
$$P = K \mu \qquad\qquad\qquad \text{for } \mu < \mu_0$$

Table 1
Elastic Constants For The Kirghizia
Limestone Model

P wave velocity:	6000 m/sec
S wave velocity:	3750 m/sec
Poisson's ratio:	0.18
Density:	2.7 gm/cm^3
Bulk modulus:	466 kb
Shear modulus:	380 kb

where P is the mean stress, K is the bulk modulus, μ is the reduced compression ratio, and B and μ_o are constants of the fit having magnitudes of 1219 kb and 0.0022, respectively. Previous studies (Duff *et al.*, 1987) have shown that the omission of an energy dependent term in the calculation of mean stress in the rock outside the cavity has a negligible effect on the calculated velocities and displacements at ranges corresponding to peak stresses below 1 kb.

Since no material properties data were available for the rock strength at the Kirghizia site, it was assumed that this rock would be somewhat similar to the hard limestone at the Silver City site, for which such data were available (Chitty and Blouin, 1993). The Peyton failure surface algorithm for rock, discussed in detail in Rimer *et al.* (1984), which models the dependence of strength upon the third deviatoric invariant, was used here to model the limestone strength behavior. In the formulation, the strength in pure shear, τ, was assumed to depend upon mean stress as given by an exponential of the form

$$\tau = \tau_o - \tau_i \, e^{-P/\tau_d}$$

where the coefficients τ_o, τ_i, and τ_d, were given magnitudes of 3.863, 3.713, and 4.4678 kb, respectively, for these limestone calculations. From this expression, the maximum stress difference in any other stress state can be determined using the Peyton algorithm. (For the spherically symmetric

calculations discussed here, the only relevant stress states are compression and tension.) Stress difference in compression is given as 2.35 τ, while its value in tension is 1.5 τ. Note that at zero P, $\tau = \tau_0 - \tau_i = 0.15$ kb, while at large P, the expression asymptotes to $\tau = \tau_0$. These values of τ correspond to stress differences in compression of 0.3525 and 9.08 kb, respectively. Deviatoric stresses are calculated using Hooke's Law unless these stresses exceed this failure surface (yield). In that event, they are adjusted (reduced) to lie on the failure surface at the same mean stress using the nonassociated flow rule (radial return).

The results of interest in these calculations are most sensitive to the shear strength of the rock. For tamped events, higher strength results in lower displacements and lower RDP. For relatively decoupled cavity events, the strength, particularly at low mean stresses corresponding to the pre-shot in situ rock stress, determines the scaled cavity radius for full decoupling. Strength values at higher pressures may be expected to be relatively consistent from site to site. However, the strength at low pressure can vary dramatically in the same rock type from site to site as a result of microfracturing and macrofracturing patterns in the rock. Since both the 2.88 m and 4.92 m cavities at Kirghizia appear to be fully decoupled for a 1.0 ton explosive yield, these data provide a lower bound to the strength of the limestone at lower pressures which is very close to that discussed above.

The results of interest are, in general, less sensitive to parameters of the equation of state of the explosive detonation products. The chemical explosive used for the Kirghizia 1.0 ton events was described as ammonium nitrate having a density of roughly 1.6 gm/cm^3. Since this explosive has not been well characterized, most of the simulations were made for the well-characterized TNT explosive, which has a density of 1.63 gm/cm^3. The JWL EOS for high explosives (Lee *et al.*, 1973) was used to model the explosive detonation and to compute the cavity pressure variation with time. Material properties for TNT for this EOS may be found in Dobratz (1981). Several calculations were also made using a modified TNT EOS, intended to better simulate the ammonium nitrate (AN) explosive. This AN simulant had the same initial density, a much lower Chapman-Jouguet

Pressure (121 kb) compared to TNT (210 kb), and a lower detonation velocity, 5270 m/sec, versus 6930 m/sec for TNT. In general, calculations with this AN model gave decoupling factors (tamped/cavity) which were very similar to those calculated using TNT. However, the AN decoupling factors did not show the complicated structure at frequencies of 50-150 Hz which were seen for the TNT results to be discussed later in this report. For the tamped cavity case, the low frequency RDP for the AN simulant was roughly 10 percent smaller than for the TNT case.

For the decoupled cavity events, shock wave propagation in the air surrounding the chemical explosive was modeled using an air EOS originally developed at the Air Force Weapons Laboratory. This EOS has been used in a number of earlier decoupled cavity studies such as Stevens *et al.* (1991a). For the simulations of decoupled nuclear events, the explosive energy was uniformly distributed in a volume of air large enough to produce an initial pressure of roughly 1000-1500 kb using this equation of state. However, for the tamped nuclear case, the initial cavity in the calculations was made large enough to vaporize roughly 70 tons of rock per kiloton of explosive yield. Using an ideal gas equation of state for the cavity materials, this resulted in an initial cavity pressure of ~650 kb. The calculated values of RDP were found to be less sensitive to these simplifying assumptions than to the poorly known material properties of the limestone site.

Spherically symmetric finite difference calculations were carried out to simulate the seismic source functions corresponding to the 1.0 ton Kirghizia tests for the tamped and 2.88 m radius cavity configurations. For this and all subsequent cavity simulations, the Lamé elastic solution was used in the calculations to insure that the decoupled cavities were in equilibrium with the 77 bar overburden pressure at the onset of the simulations. For the material model described above, the limestone surrounding the 2.88 m radius cavity did not fail in shear or tension and, consequently, this case provides a good test of the low pressure equation of state employed in these simulations. The peak displacements and velocities as a function of range resulting from this cavity simulation are plotted in Figure 17, where they are compared with the observed data from this test.

Figure 17. Comparison of simulated and observed peak displacements (left) and velocities (right) for the 1.0 ton Kirghizia decoupled test in the center of the 2.88m radius spherical cavity.

It can be seen that the simulated peak displacements (left) lie somewhat below the data in this case, although the predicted and observed attenuation rates are in good agreement. The corresponding computed peak velocities (right), on the other hand, lie well above the mean of the observed data and show a significantly lower rate of attenuation with distance. In fact, if this test was indeed fully decoupled, then the observed $r^{-1.75}$ attenuation rate is inconsistent with the theoretical elastic solution, and must be associated with some anelastic decay mechanism which is not modeled in these calculations. However, even in the absence of this discrepancy between theoretical and observed attenuation with distance, it is clear from the close-in comparison at a range of 10 m that the theoretical simulation is significantly overestimating the observed peak velocity levels for this test.

Similar comparisons for the 1.0 ton tamped test are presented in Figure 18 where, once again, the calculations are seen to be in better agreement with the observed peak displacements than with the corresponding observed peak velocities. This tendency for the simulations to underestimate the peak displacements and overestimate the peak velocities suggests that the limestone material model being employed in these calculations has a shear strength which is too large. However, the reasonable agreement between the calculated and observed peak displacements for these two tests suggests that this model should provide an adequate description of the low frequency decoupling efficiency, which is of primary interest for seismic monitoring purposes.

The simulated decoupling as a function of frequency for the 1.0 ton HE test in the center of the 2.88 m radius spherical cavity is shown in Figure 19 where it is compared with both the corresponding experimental estimate from Figure 15 and the theoretical prediction for a 1 ton nuclear explosion in that same cavity. It can be seen that the theoretical HE simulation predicts a maximum low frequency decoupling factor of about 25 in this case, in good agreement with the estimate obtained from the measured data on that test. The agreement between the simulated and observed frequency dependence of the decoupling factor is less satisfactory in that it appears that the simulation overestimates the corner frequency of the tamped test by a significant amount. This result is consistent with the
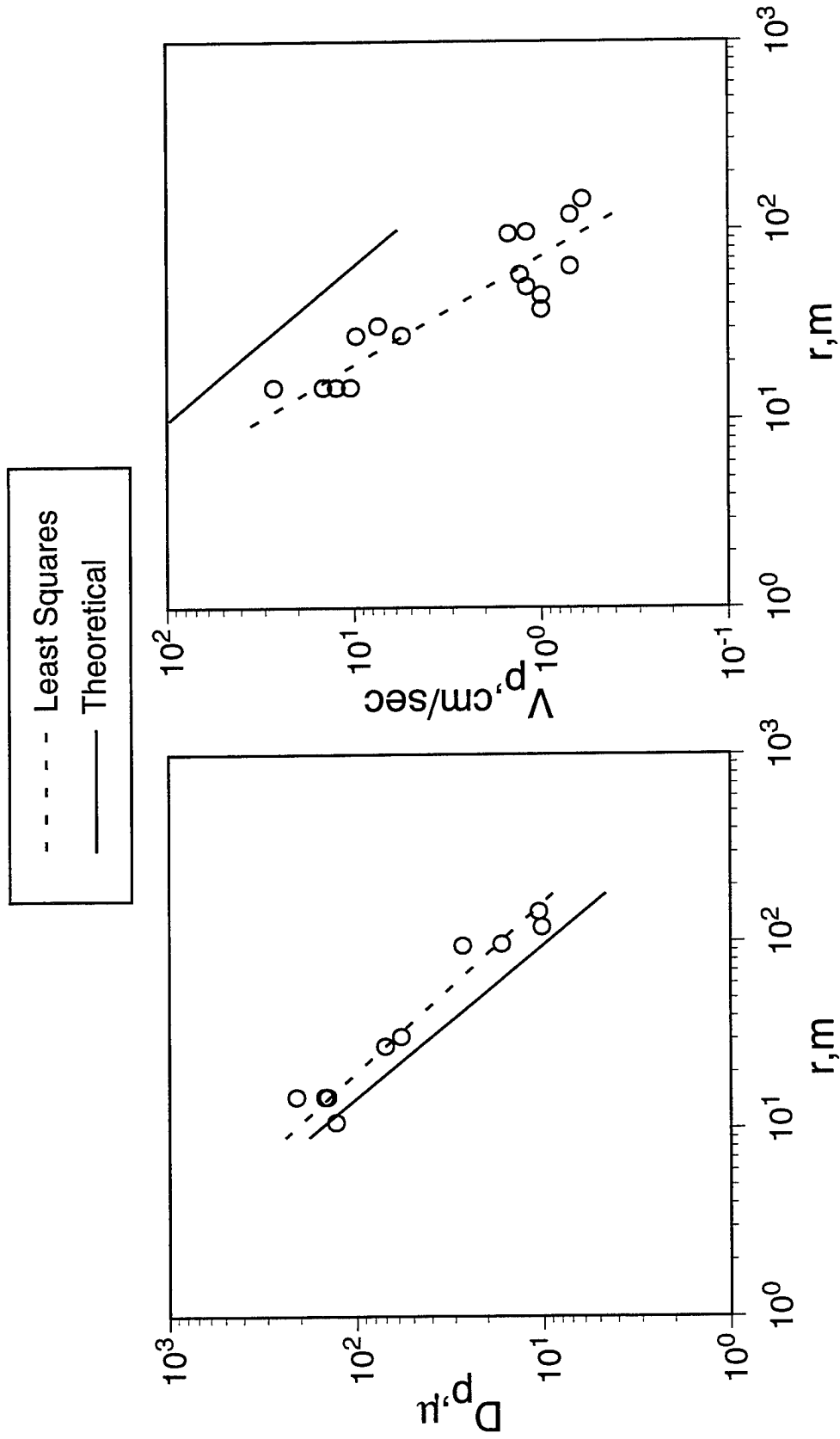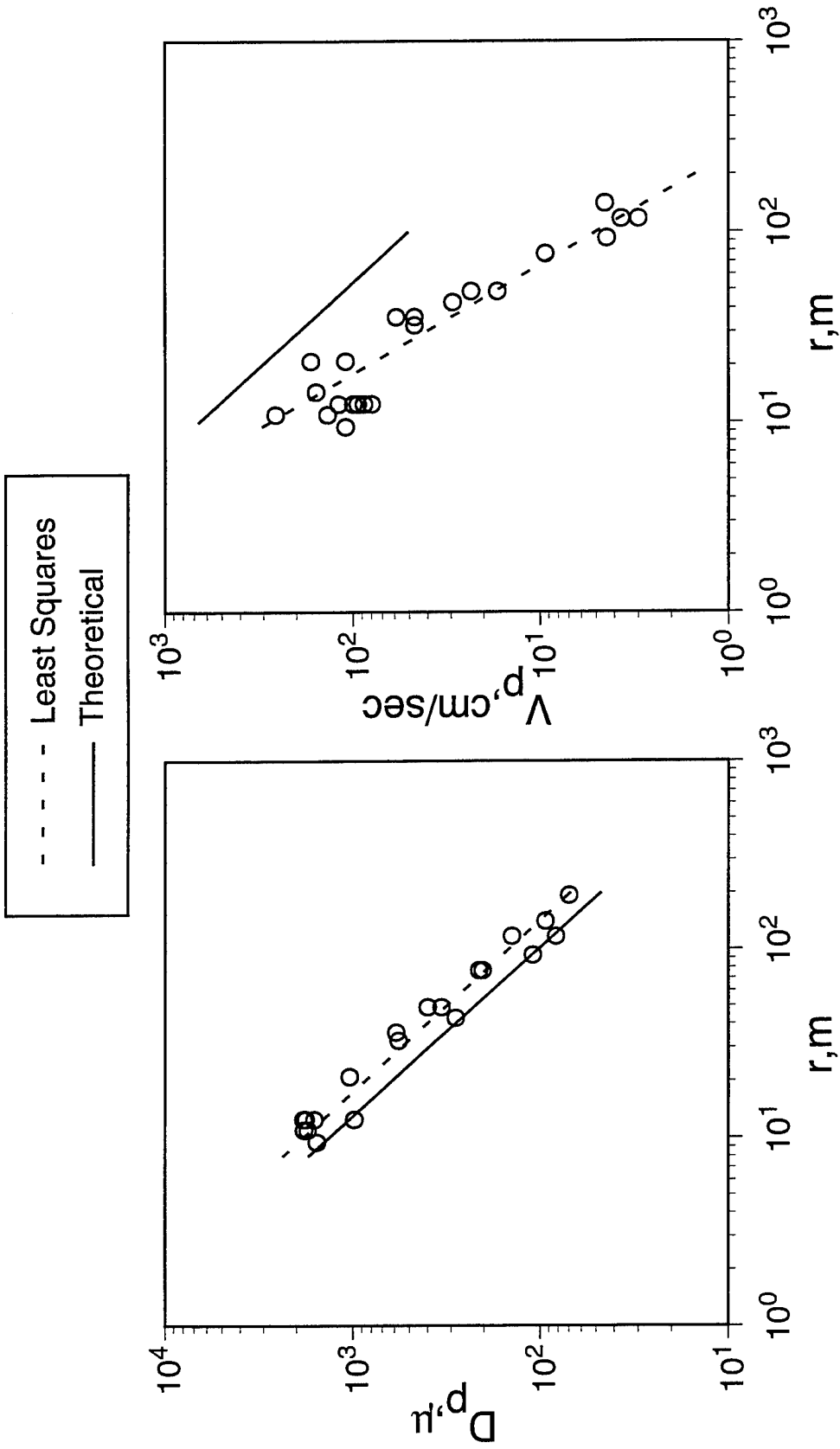
Figure 18. Comparison of simulated and observed peak displacements (left) and velocities (right) for the 1.0 ton Kirghizia tamped test.
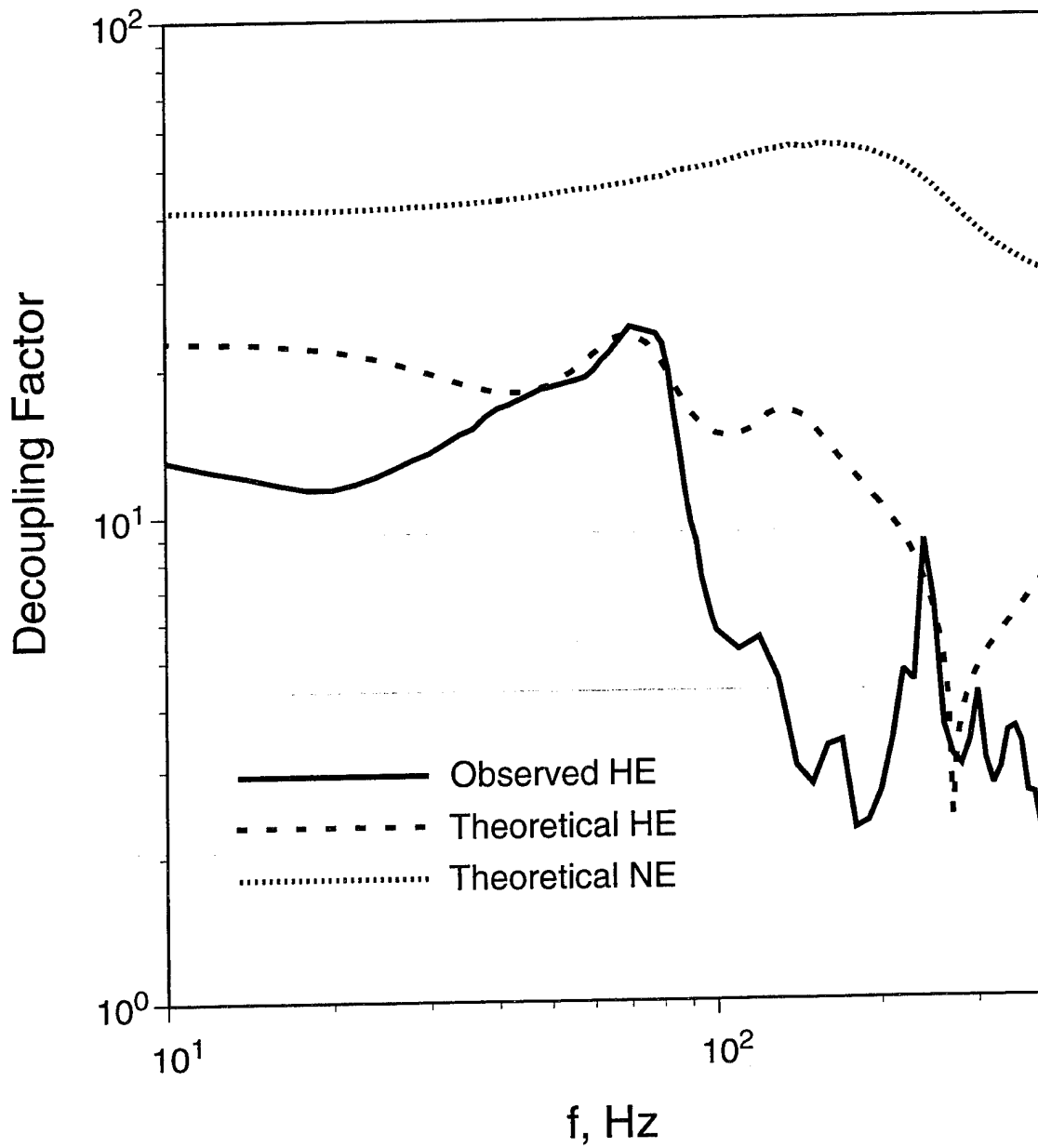
Figure 19. Comparison of observed and theoretical frequency dependent decoupling factors for 1 ton explosions in a 2.88m radius spherical cavity in Kirghizia limestone.

peak motion comparisons shown in Figures 17 and 18 and provides further evidence that the limestone model being used in the theoretical simulations is too strong. It follows that additional work on the equation of state of limestone will be required in order to define a completely satisfactory simulation capability for applications to the higher frequency characteristics of the seismic sources for such tests.

The dotted line on Figure 19 shows the corresponding frequency dependent decoupling predicted for a 1.0 ton nuclear source in this same cavity. It can be seen that for this source, the maximum low frequency decoupling factor is predicted to fall in the range of 50-60, which is significantly larger than the corresponding HE decoupling factor of 25 and close to the nominal factor of 70 quoted for the STERLING experiment. This difference between predicted decoupling factors for HE and nuclear sources of the same yield in a fixed cavity has been noted before from theoretical simulations of decoupling in salt (Glenn and Goldstein, 1994; Murphy et al., 1996). Figure 20 shows a comparison of our predicted low frequency decoupling factors for HE and nuclear sources in limestone (left) and salt (right), plotted as a function of scaled cavity radius up to the scaled radii where full decoupling is predicted. It can be seen that the theoretically predicted differences between the HE and nuclear decoupling factors are qualitatively similar for these two media, although the absolute levels of decoupling efficiency do appear to show some medium dependence.

In summary, the Russian Kirghizia HE decoupling test series has provided much new information regarding the dependence of decoupling efficiency on scaled cavity size and shape for explosions in a hardrock medium. Analyses of seismic data recorded from these tests indicate that HE explosions at a depth of 290 m in that limestone are essentially fully decoupled in spherical cavities with scaled cavity radii larger than about 27 $m/kt^{1/3}$ and that low frequency decoupling effectiveness under such conditions is approximately independent of cavity shape for roughly cylindrical cavities with length to width ratios of 6 or more. Spectral analyses of the available waveform data indicate a maximum low frequency decoupling factor of about 25 for fully decoupled HE tests in this
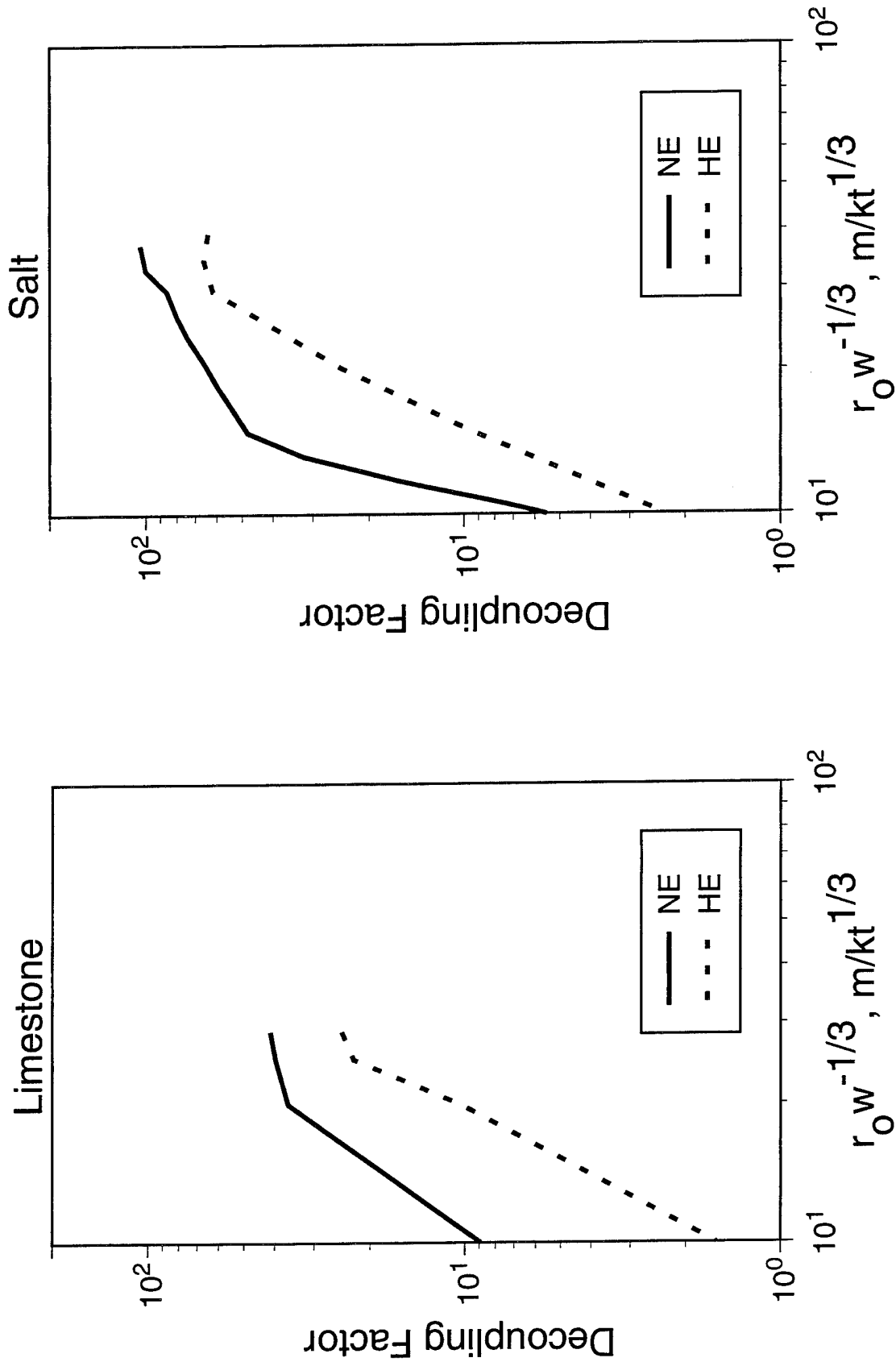
Figure 20. Comparison of simulated low frequency decoupling factors for HE and nuclear explosions in limestone and salt, plotted as functions of scaled cavity radius.

limestone, and theoretical simulation results suggest that the corresponding nuclear decoupling factor would be expected to be in the range of 50-60.

3. AZGIR WATER-FILLED CAVITY EXPERIMENTS

3.1 Overview

On July 1, 1968 the Russians detonated a 27 kt tamped nuclear explosion at a depth of 597 m in salt at their Azgir test site located within the central portion of the Caspian depression of the Russian platform (Cf. Figure 1). This explosion produced a stable, roughly spherical cavity which subsequently filled with water which flowed in through the emplacement hole from the pierced water table above the cap rock. A post-test downhole survey indicated that this cavity had a maximum horizontal radius of 32.5 m and a total volume of 101,000 m^3. This total volume is equal to that which would be associated with a purely spherical cavity with a radius of 28.9 m, which is about 10% smaller than the observed maximum radius in the horizontal plane. During the period from April 1975 to January 1979, the Russians conducted a series of six nuclear explosions in this water-filled cavity. According to Kitov et al. (1995), the primary objective of these experiments was to investigate a procedure for producing trans-plutonium elements in experimental amounts. A secondary objective was to evaluate the possibility of using such source configurations to produce efficient and repeatable sources of seismic waves for use in the dynamic characterization of seismogenic zones in the earth. Moreover, since the cavity conditions were monitored after each test, this series of experiments also provided valuable information regarding the feasibility of using such cavities for multiple explosive tests. The results of these latter investigations were summarized in our previous report (Murphy et al., 1994).

The source parameters of the seven nuclear explosions conducted in emplacement hole A2 at Azgir are listed in Table 2, where it can be seen that the yields of the water-filled cavity explosions varied over a factor of

50, ranging from 0.01 to 0.50 kt. Now a 28.9 m radius, air-filled cavity at a depth of 585 m in salt would be expected to decouple a 1.3 kt explosion to the same degree as that achieved for the U.S. STERLING explosion. It

Table 2
Source Parameters For Azgir Water-Filled Cavity Tests

Emplacement Coordinates: 47.9086N, 47.9119E

Event	Date	Origin Time, UT	Depth, m	Yield, kt
A2	7-01-68	04 02	597.2	27
A2-2	4-25-75	05 00	582	0.35
A2-3	10-14-77	06 59 59.100	587	0.10
A2-4	10-30-77	06 59 59.069	586.2	0.01
A2-5	9-12-78	04 59 58.494	585	0.08
A2-6	11-30-78	04 59 58.929	586	0.06
A2-7	1-10-79	08 00	590	0.50

follows that if this cavity had been air-filled, all of the A2 cavity tests would have been fully decoupled and the associated seismic signals would have been well below the teleseismic detection threshold. In fact, however, the two largest of these cavity explosions (i.e., A2-2 and A2-7) were detected at teleseismic distances and have been assigned m_b values in the 4.0 to 4.5 range. Since a fully tamped 1 kt explosion in salt at Azgir corresponds to an m_b value of 4.5 or less (Murphy and Barker, 1994), it follows that these cavity tests were not decoupled and, in fact, seem to show enhanced coupling over some frequency bands, more consistent with what would be expected for explosions in water (Evernden, 1970). Nevertheless, their wide range in energy release at a fixed detonation point provides a unique opportunity to examine the seismic source characteristics of such explosions.

3.2 Seismic Data Analysis

Seismic data from this series of explosions in Azgir emplacement hole A2 were recorded at 28 stations located in the near-regional distance range extending from about 1 to 175 km. Both vertical and horizontal radial component data were recorded at stations located within 20 km of ground zero and full, three-component data sets were recorded at the more distant stations. Photographic recordings from the tamped explosion A2 and the first four of the water-filled cavity tests (i.e., A2-2, A2-3, A2-4, A2-5) have now been collected and carefully digitized at IDG using standardized procedures described by Kitov *et al.* (1994). Most of these data were digitized at sampling rates of 200 samples/second or higher, which provides more than adequate resolution of the highest frequency components which can be reliably recovered from this recording medium. At a number of stations, data were recovered from most or all of these tests on a common instrument, thereby providing a basis for direct comparisons in which the propagation paths and recording parameters are held constant. These data were presented and discussed in some detail in our previous report (Murphy *et al.*, 1994) and, therefore, in this report we will focus exclusively on analyses of the recordings at three of the closest stations (i.e., 1.17, 1.71 and 7.8 km) for which the usable bandwidths of the data are wide enough to examine the most important seismic source characteristics of these tests.

The vertical component displacement data recorded at a distance of 1.17 km from the Azgir tamped and selected water-filled cavity tests are presented in Figure 21, where they have been arranged in order of decreasing yield from top to bottom. It is evident from this display that the source corner frequency of the tamped test is much lower than those of the cavity tests, consistent with the large differences in yield. It can also be seen that the character of the seismic signals recorded from the cavity tests changes as a function of yield, with the signals becoming progressively more complex as the yield decreases. This is particularly evident for the lowest yield A2-4 recording which shows a prolonged ringing which is not evident in the recordings from the larger yield cavity shots. These qualitative observations are confirmed in Figure 22, which shows a

41

A2
Tamped
27 kt

A2-2
0.35 kt

A2-3
0.10 kt

A2-5
0.08 kt

A2-4
0.01 kt

.25 sec
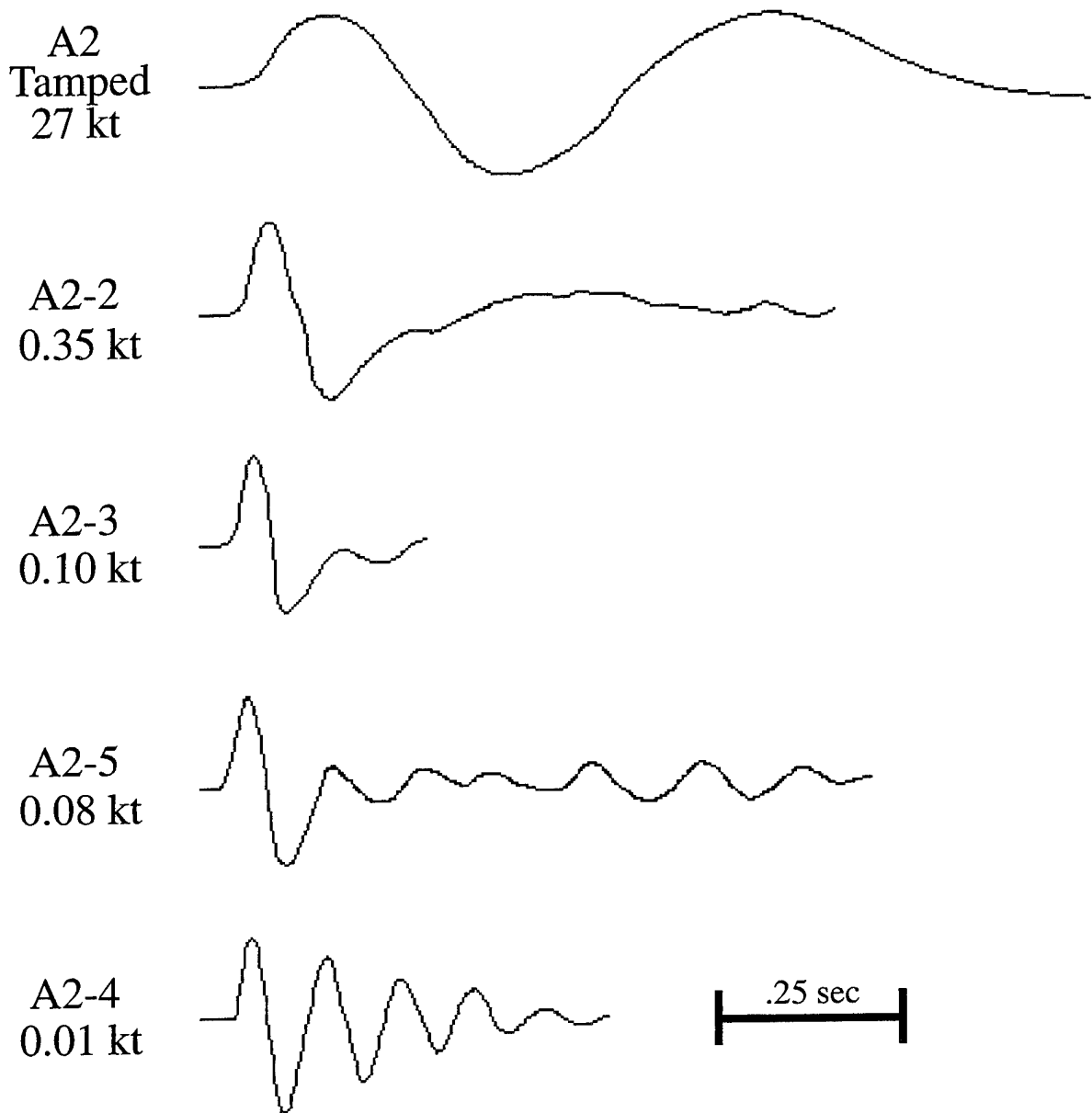
Figure 21. Comparison of vertical component seismic data recorded from the Azgir tamped and water-filled cavity explosions at a range of 1.17 km.
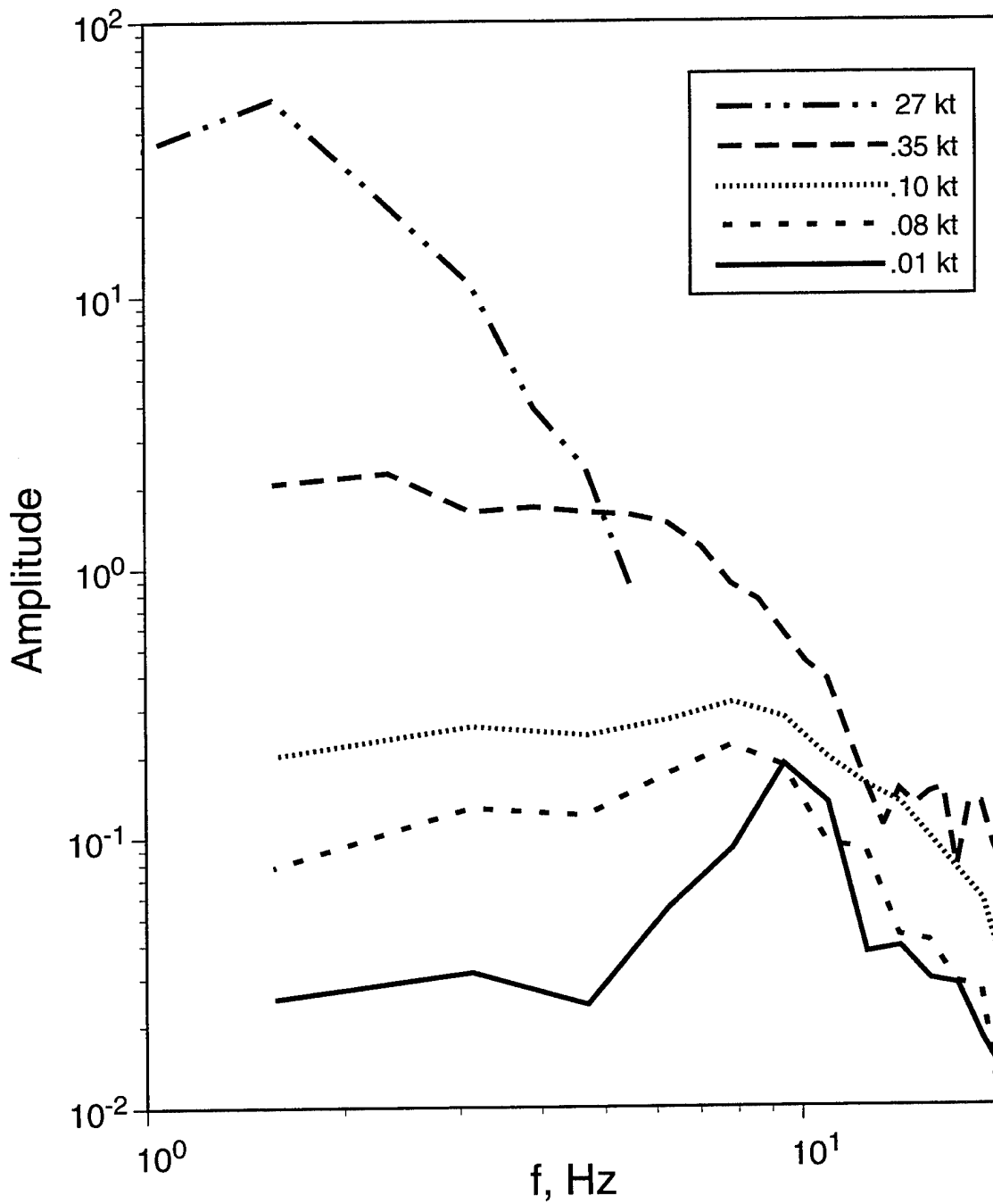
Figure 22. Comparison of displacement spectra computed from vertical component data recorded from the Azgir tamped and water-filled cavity tests at a range of 1.17 km.

comparison of the spectra computed from the signals in Figure 21. Note that because of the dynamic range limitations of the hand-digitized data, the spectrum for the tamped A2 explosion is only considered to be reliable below about 5 Hz, because of its low corner frequency, while the cavity test spectra are estimated out to 20 Hz. Note also that the spectrum for the 0.01 kt cavity test shows a strong resonance peak at around 10 Hz, consistent with the previously noted oscillatory nature of the corresponding waveform in Figure 21. The spectra derived from the recordings of these four cavity tests at the 1.71 and 7.8 km stations are plotted in Figures 23 and 24, respectively. Comparing the spectra of Figures 22-24, it can be seen that the spectral shapes for any one explosion are quite similar at all three distances, which suggests that the propagation path effects are not very pronounced at these near-field distances.

The band-limited spectra corresponding to the tamped 27 kt A2 event recordings at the three distances are shown in Figure 25 where they have been normalized to a common low frequency level for comparison purposes. Here, the low frequency (f < 1 Hz) levels have been approximated from the higher frequency data by determining the best-fitting Mueller/Murphy source function for the three individual spectra corresponding to this tamped explosion in salt. Once again, it can be seen that the three spectra are very similar in shape, suggesting that frequency dependent propagation path effects may be of second order importance in this case. If this were strictly true, the tamped explosion spectra at these three stations could be simply cube-root scaled to the yields of the cavity tests and used to compute spectral ratios which would then be equal to the frequency dependent cavity/tamped source spectral ratios. The results of applying this approximation to the data of the four cavity tests are shown in Figure 26, where it can be seen that the cavity/tamped spectral ratios obtained for a given explosion at the three distances are reasonably consistent, suggesting that they may indeed represent useful approximations to the corresponding source spectral ratios. Figure 27 shows the results of logarithmically averaging these three estimates of the source spectral ratio for each cavity test. It can be seen from this figure that, to this degree of approximation, it can be concluded that the 0.35 kt A2-2 water-filled cavity test shows enhanced coupling at low frequencies with respect to that
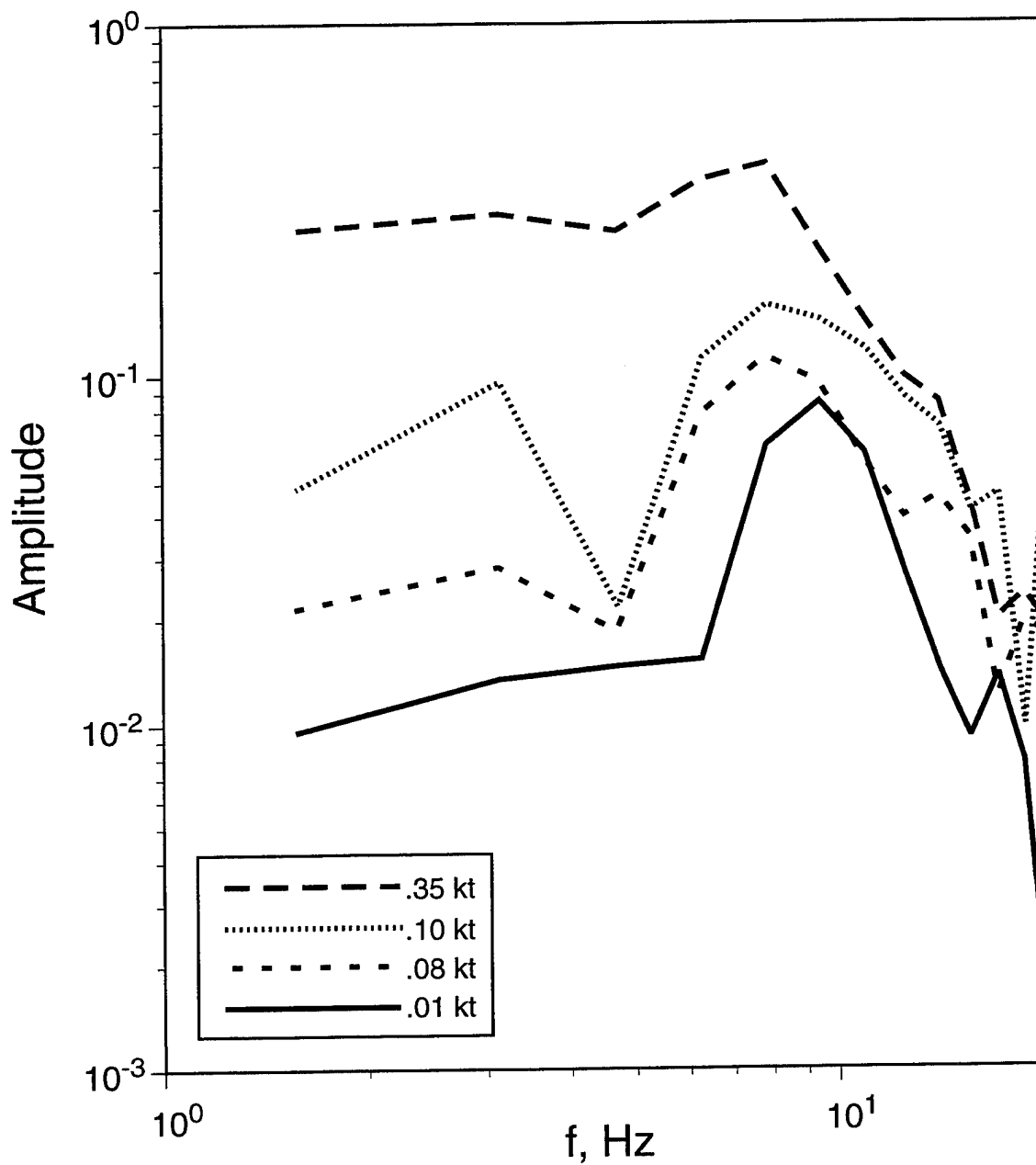
Figure 23. Comparison of displacement spectra computed from vertical component data recorded from the Azgir water-filled cavity tests at a range of 1.71 km.
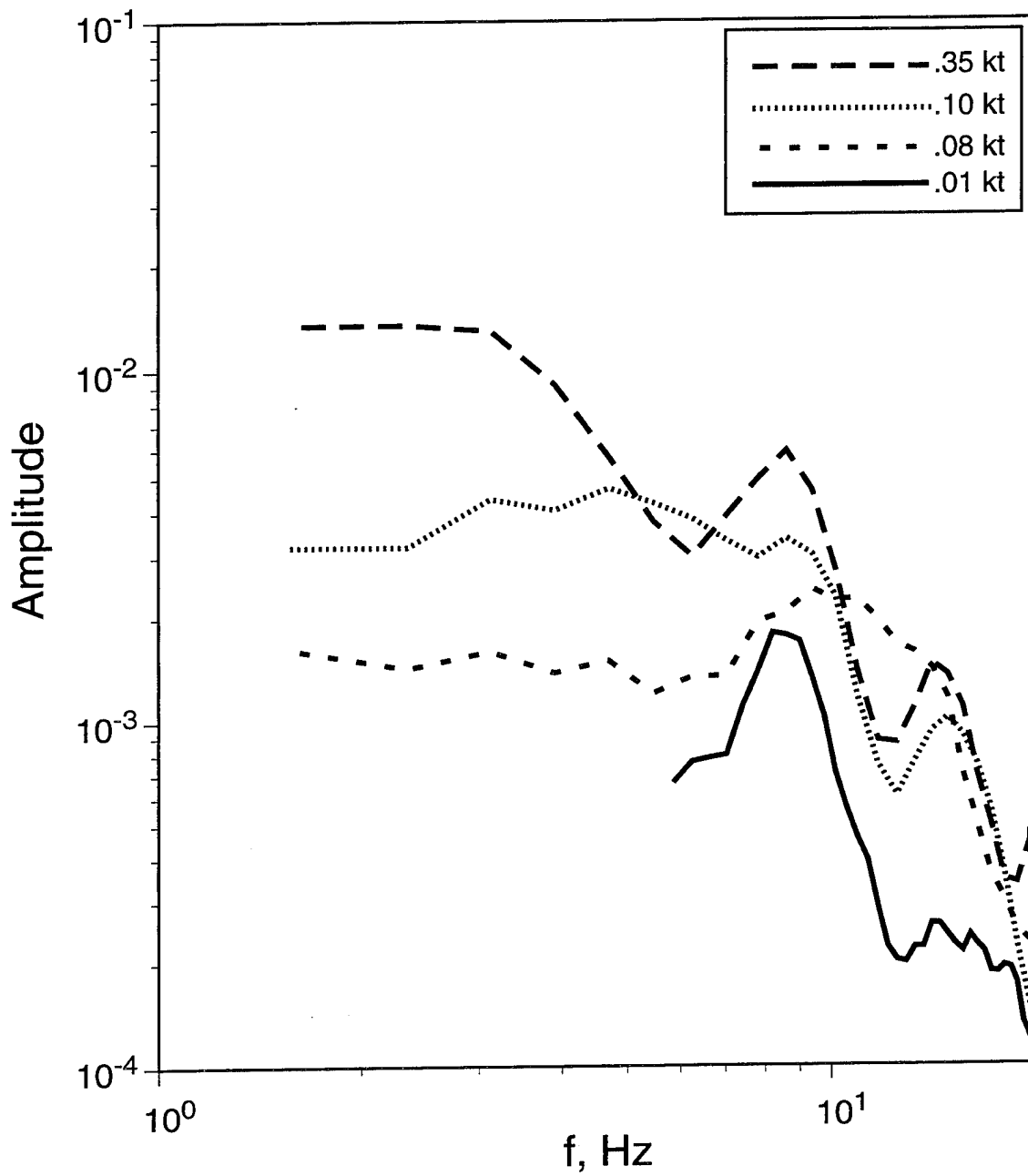
Figure 24. Comparison of displacement spectra computed from vertical component data recorded from the Azgir water-filled cavity tests at a range of 7.8 km.
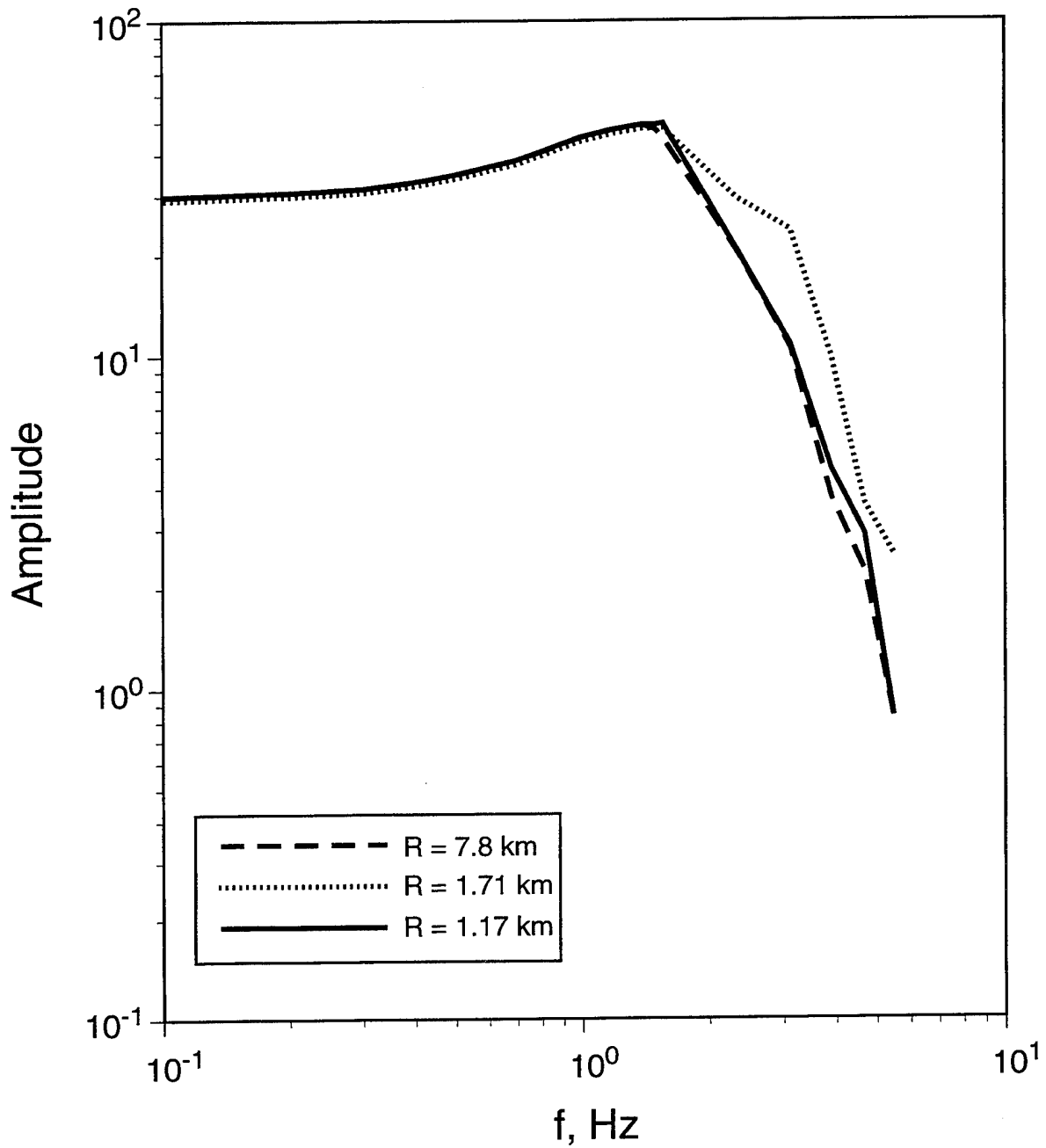
Figure 25. Comparison of amplitude-normalized displacement spectra corresponding to the vertical component recordings of the Azgir A2 tamped 27 kt explosion at each of the three distances.
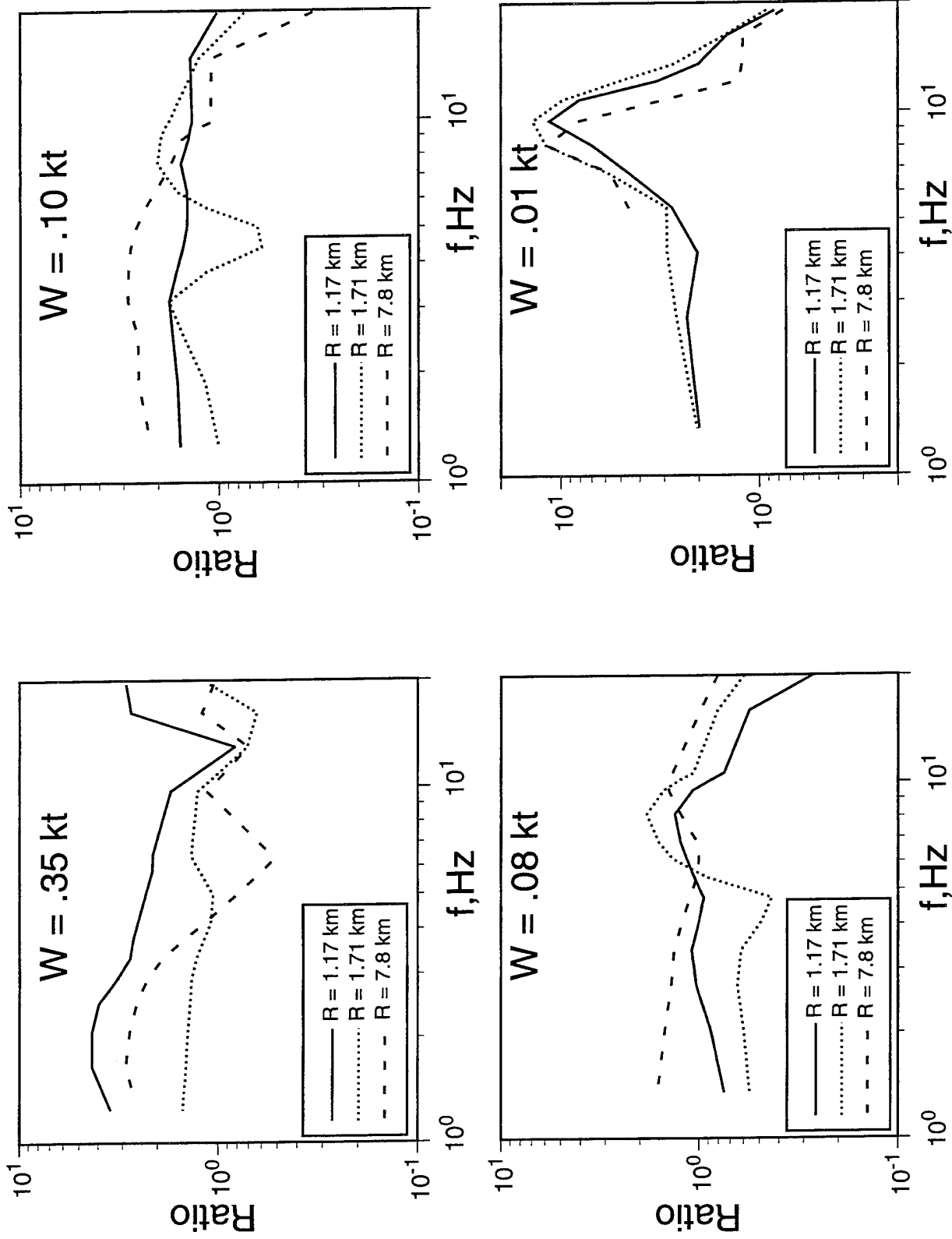
Figure 26. Individual cavity/tamped source spectral ratios estimated from the observed Azgir near-regional seismic data by cube-root scaling the observed tamped spectra to the yields of the water-filled cavity tests.
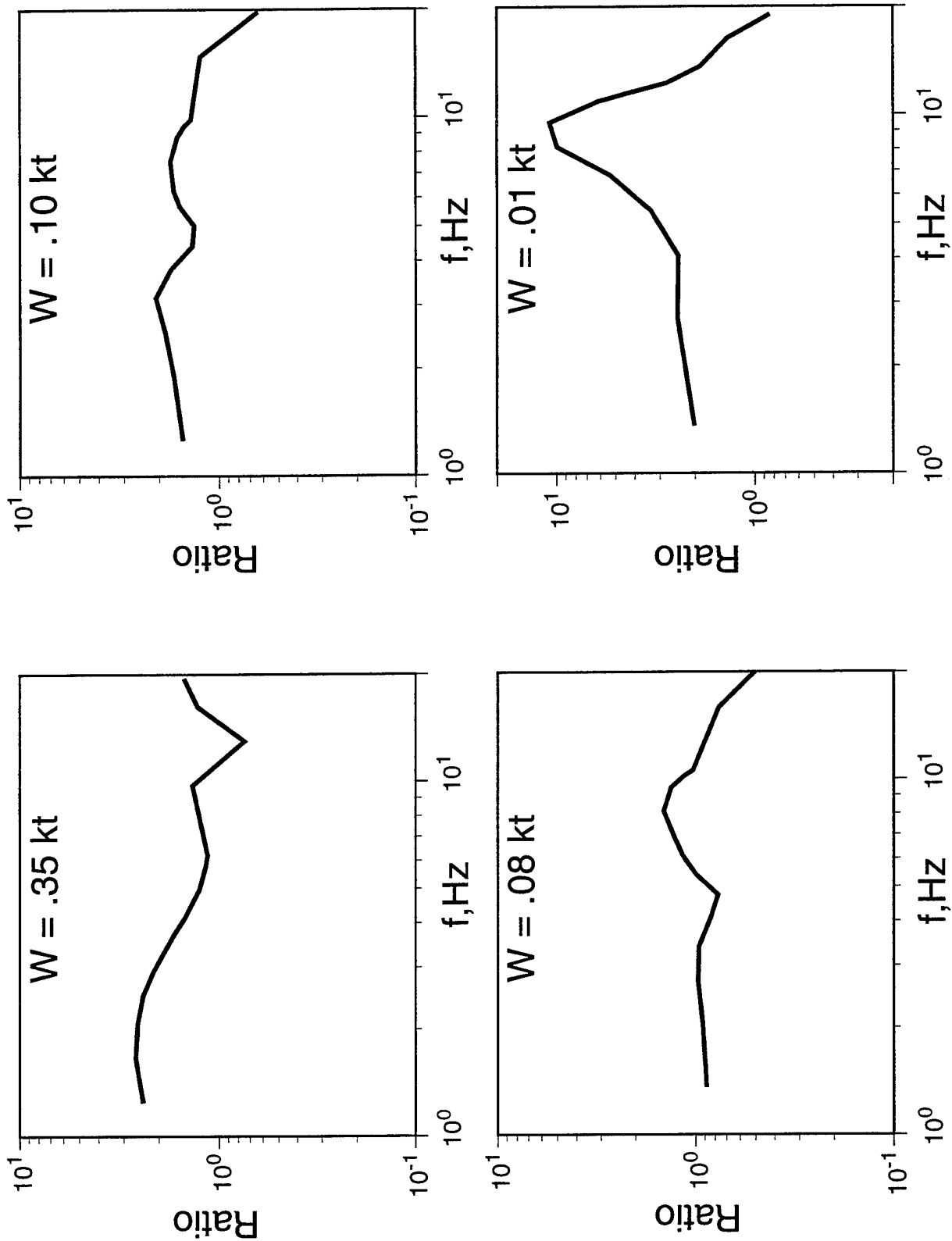
Figure 27. Average cavity/tamped source spectral ratios estimated from seismic data recorded from the Azgir tamped and selected water-filled cavity tests at three different near-regional stations (1.17, 1.71, 7.8 km).

expected from a tamped explosion of the same yield in salt, while the 0.10 kt A2-3 and 0.08 kt A2-5 cavity tests appear to be roughly comparable to tamped shots of those yields in salt over the entire frequency range of observation. The 0.01 kt A2-4 cavity test spectral ratio, on the other hand, shows a pronounced resonance in the band around 10 Hz, where the overshoot of the low frequency level amounts to a factor of 5 or more. Thus, the source spectral ratios corresponding to these four cavity tests show some pronounced yield dependencies which should correlate with differences in the seismic source generation mechanisms between these different explosions.

An alternate way of analyzing these water-filled cavity test data has been described by Sultanov (Kitov *et al.*, 1995). In this approach, peak velocity prediction equations determined from statistical analyses of a large sample of data recorded from tamped Azgir explosions were used to estimate the peak velocities to be expected from tamped explosions in salt having yields equal to each of the four cavity tests. Ratios of the observed to predicted peak velocities were then computed for each test and averaged to obtain measures of relative coupling efficiency. Sultanov found that these computed peak velocity ratios ranged from about 3 to 5, with the largest ratio corresponding to the lowest yield 0.01 kt A2-4 test. Sultanov therefore concluded that all the water-filled cavity explosions show a significantly increased seismic efficiency relative to tamped explosions in salt of the same yield. Given the scatter in the spectral ratio data from the various stations shown in Figure 26, such a conclusion is not necessarily inconsistent with the average source spectral ratio estimates presented in Figure 27. However, there are reasons to be somewhat cautious in the interpretation of the peak velocity ratio results. In the first place, the peak velocity prediction equations being used as a reference were derived from data recorded from much larger explosions which were detonated over a range of burial depths and, consequently, their extrapolation to lower yield explosions at a fixed depth are subject to some significant uncertainty. Furthermore, comparisons of the peak velocities observed from the 27 kt tamped A2 event with those observed from the cavity tests indicate that the dominant frequencies of the peaks vary quite widely over this range in yields. Consequently, it is not at all obvious how to interpret these peak

velocity ratios in terms of the spectral ratios of Figure 27. It follows that some uncertainties remain regarding the relative low frequency seismic efficiencies of these water-filled cavity tests with respect to those expected from tamped explosions of those yields in salt. However, the strong yield dependence of the seismic source spectra corresponding to these different cavity tests has been firmly established, and it is this feature of the data which will be investigated in detail in the following theoretical simulation analysis.

3.3 Theoretical Simulation Analysis

The theoretical simulation of the seismic motions produced by nuclear explosions of different yields in the Azgir water-filled cavity is obviously complicated by the nonlinear interactions between the shock effects in both the water and the surrounding medium. Kostuchenko (Kitov et al., 1995) derived an analytic approximation to the seismic source function for such explosions by establishing a low frequency seismic yield equivalence factor which relates the actual yield of the cavity explosion to the yield of an "equivalent" tamped explosion in salt. While this model does seem to provide some insight into the relative low frequency coupling efficiency of these tests, it is quasi-static in nature and, therefore, can not account for the dynamic shock effects in the water-filled cavity which appear to be related to the strong yield dependence of the seismic sources identified previously in Figure 27. Consequently, in the following analysis we will focus on the results of a series of nonlinear finite difference simulations which explicitly account for such dynamic effects.

Before beginning the discussion of the specific finite difference calculations, it will be useful to briefly review the phenomenology associated with nuclear explosions in water. According to Pritchett (1971), near the burst point the internal energy imparted to the water by the explosion is sufficient that, upon expansion, the water will vaporize. For a 1 kt nuclear explosion, this vaporization will result in the generation of a steam bubble with an initial radius of about 3.7 m and an internal pressure of about 80 kilobars. In the open ocean, this high pressure bubble will

subsequently expand until the internal pressure decreases to a little below overburden pressure (i.e., it overshoots the equilibrium point), whereupon it will rebound and collapse down to a minimum volume, where it is once again brought to a halt by the high internal pressure. At an overburden pressure of 60 bars, this initial expansion cycle results in a maximum bubble radius of about 37 m, or an expansion of bubble volume by about a factor of 1000. Once the bubble collapses to its minimum volume, the internal pressure is once again much higher than the overburden, and a new expansion cycle begins. This cycle of expansion and collapse would continue indefinitely in the absence of dissipation mechanisms. However, significant energy is in fact dissipated in each cycle due to Taylor instability and turbulence at the steam/water interface at bubble minimum and, as a result, only three cycles of expansion and collapse are observed from underwater nuclear sources. A pressure pulse is emitted at the end of each contraction phase, when the bubble is at minimum volume, and this constitutes the "bubble pulse" which is used to identify underwater nuclear explosions on hydroacoustic recordings. Of course, in the open ocean, the bubble also simultaneously rises to the surface due to its buoyancy, as it undergoes these expansion/contraction cycles.

For nuclear explosions in a water-filled cavity, the simple steam bubble dynamics described above are complicated by the dynamic interactions with the cavity wall. These effects are schematically illustrated in Figure 28 where the interactions between the expanding gas bubble and the reflected shocks from the cavity wall are shown for reference purposes. We have attempted to theoretically model this complex process with a series of one-dimensional, nonlinear finite difference simulations of explosions in a purely spherical, 28.9 m radius, water-filled cavity in salt. Lithostatic pressure at the 597 m depth of the Azgir cavity is roughly 120 bars. For the purposes of the numerical simulations to be discussed below, it was assumed that the water-filled cavity was initially pressurized at the corresponding hydrostatic pressure of about 60 bars. The Lamé elastic solution for the stresses surrounding a pressurized spherical cavity was used to determine the initial stress distribution in the salt near the cavity. Parametric studies subsequently showed that the results of the calculations
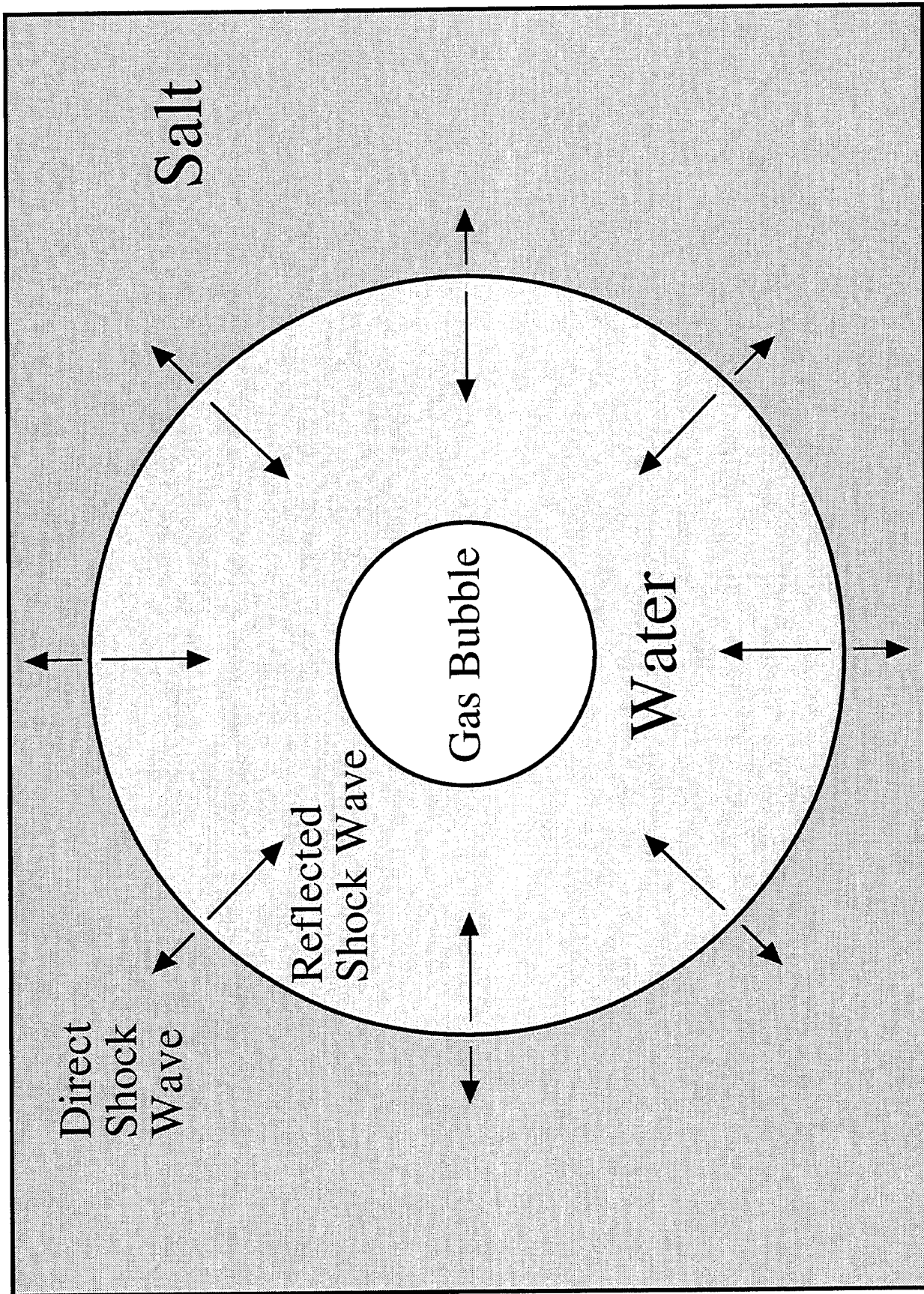
Figure 28. Schematic representation of shock wave evolution associated with a nuclear explosion in a water-filled cavity.

to be discussed here were essentially unchanged when the initial cavity water pressure was reduced to 1 bar.

The calculations were initialized with the device energy uniformly distributed in a water volume which gives an average initial pressure of 80 kilobars, sufficient to vaporize the required amount of water during the bubble expansion. Parametric calculations indicate that a substantially smaller initial bubble results in approximately the same computed spectra while a significantly larger initial bubble (a lower initial pressure) does not model the steam bubble behavior well and greatly changes the results of interest. A detailed equation of state of water, AQUA, which includes the steam tables, and most other relevant features of water behavior, was used in the calculations.

Two very different strength models were used to describe the shear behavior of the surrounding salt. The first, to be referred to as Lab Salt, assumes that the Azgir site has a failure surface similar to that measured in the laboratory on small samples of dome salt from the SALMON nuclear event. It is approximated here as a parabola in stress difference Y versus mean stress P, with a stress difference in compression of 138 bars, at zero P, and a maximum value of Y in compression of 680 bars at $P \geq 600$ bars. This model provides the "high strength bound" for the site. The second strength model, generally known as the Cherry-Rimer (CR) model, was developed to simulate the particle velocity versus time ground motion measurements made during the SALMON event (Rimer and Cherry, 1982). This model assumes that the salt has a very low strength initially and that the strength increases greatly, to the lab strength, during the strain hardening which occurs as a result of the ground motion. This model, in general, results in inelastic behavior out to far greater ranges than does the Lab Salt model. Both models have been used in a number of parametric studies of decoupling, such as those described by Stevens et al. (1991a). For the purposes of the present study it was found that, although the magnitudes of the seismic sources varied significantly between the two models, the resulting cavity/tamped source spectral ratios were relatively insensitive to the choice of model, so only the results from the simulations carried out using the CR model will be considered in the following discussion.

We will first consider the simulation of the lowest yield 0.01 kt A2-4 cavity explosion. The sequence of events in this case is summarized in Figure 29 which shows snapshots of the computed pressure as a function of range in the cavity and surrounding salt medium at different instants of time during the shock wave evolution. The dashed vertical lines on these snapshots denote the location of the cavity wall in this one-dimensional simulation. At this yield, the prompt vaporization of the surrounding water produces a steam bubble with an initial radius of about 0.8 m and an internal pressure of 80 kilobars. In Figure 29, the time dependent radius of this steam bubble is represented by the plateaus of constant pressure extending out from the origin, which coincides with the center of the cavity. This gas bubble ultimately expands to a first maximum radius of 6.2 m in about 40 msec, which is significantly smaller than the maximum radius of 8 m which would be expected for such an explosion in an unbounded water medium. This is because the water borne shock wave, which reflects from the cavity wall at about 17 msec, arrives at the expanding bubble/water boundary at about 30 msec and retards further bubble expansion. As is indicated in Figure 29, the bubble then collapses to its first minimum radius of 3.7 m at about 80 msec, whereupon it begins a second cycle of expansion and collapse. Therefore, the period of the bubble oscillation in this case is about 80 msec, giving a characteristic frequency about 12 Hz, which is close to the 10 Hz resonant frequency observed in the corresponding spectral ratio for this test shown in Figure 27. As a point of reference, the same yield test under this overburden pressure in the open ocean would be expected to produce a steam bubble which would expand to its first maximum radius of 8 m in about 100 msec and collapse to its first minimum radius in about 200 msec, giving rise to a much lower bubble pulse frequency of about 5 Hz.

The corresponding theoretical simulation of the 0.35 kt A2-2 explosion in that same cavity is summarized in Figure 30. In this case the initial vaporization radius is about 2.6 m and the computed first maximum expansion radius is only 11.7 m, as opposed to the much larger 26 m radius which would be expected in an unbounded water medium. This dramatic reduction occurs because the shock reflection from the cavity wall arrives

Figure 29. Snapshots of the computed pressure as a function of range in the cavity and surrounding salt medium at selected times of the 0.01 kt Azgir A2-4 simulation. The dashed vertical lines on these snapshots denote the location of the cavity wall.
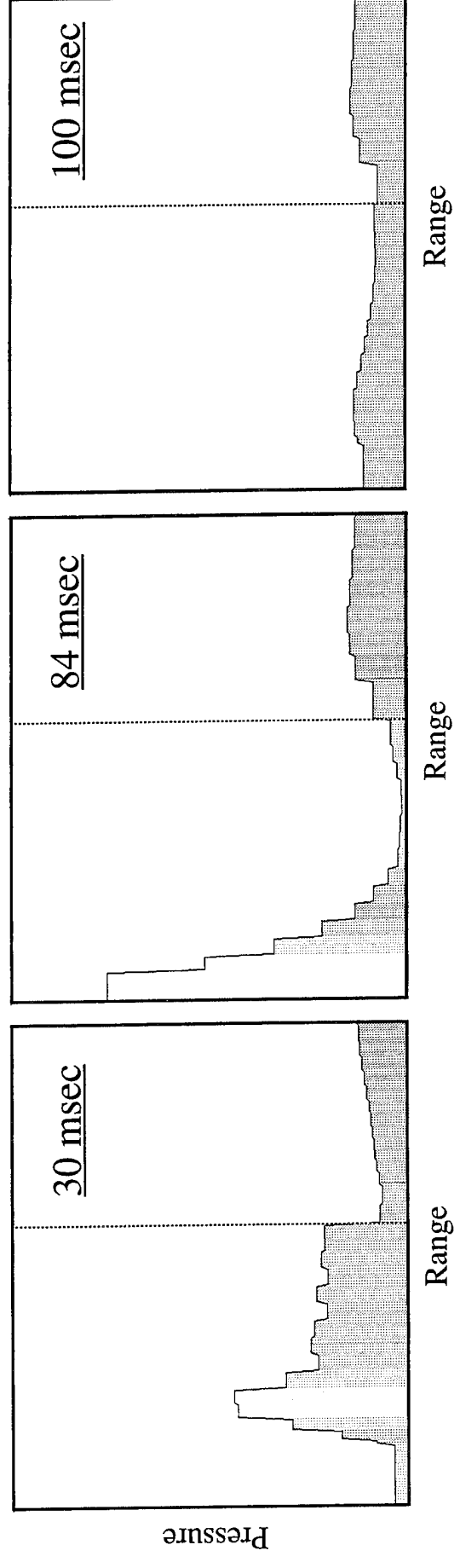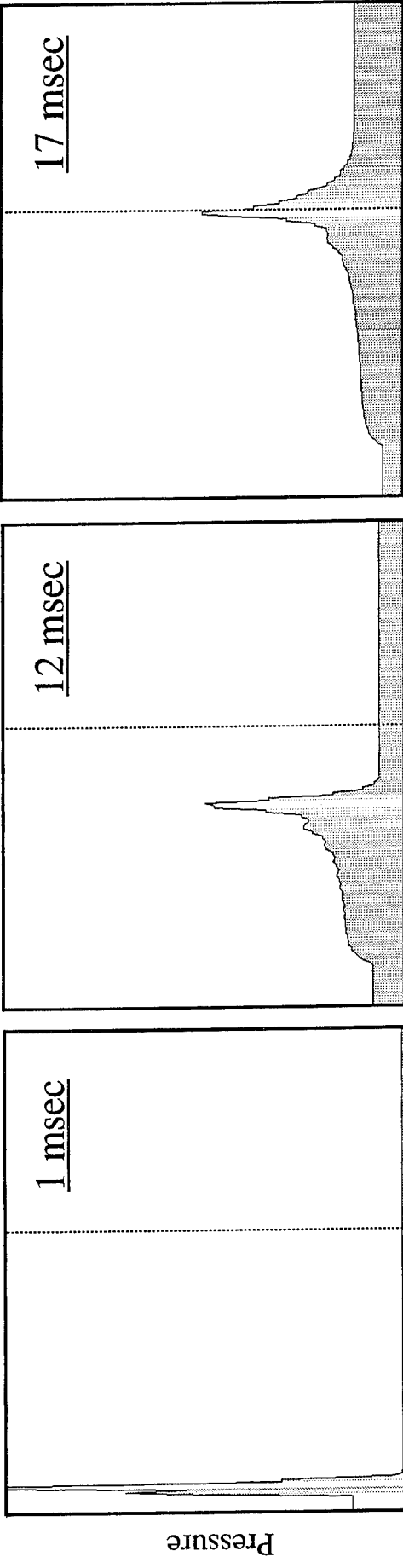
56
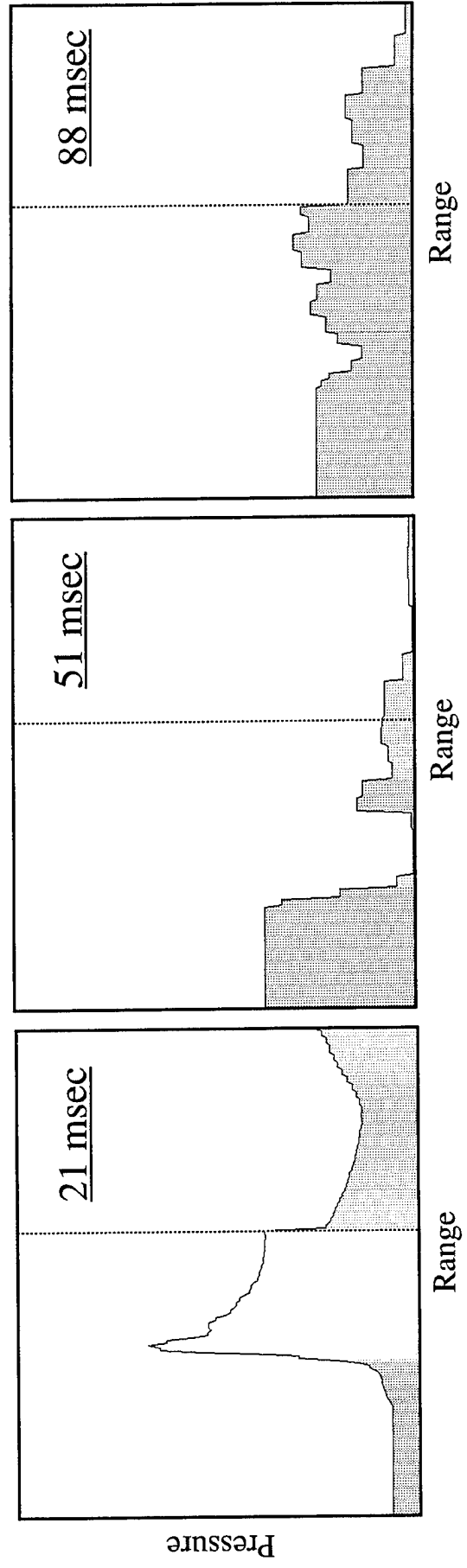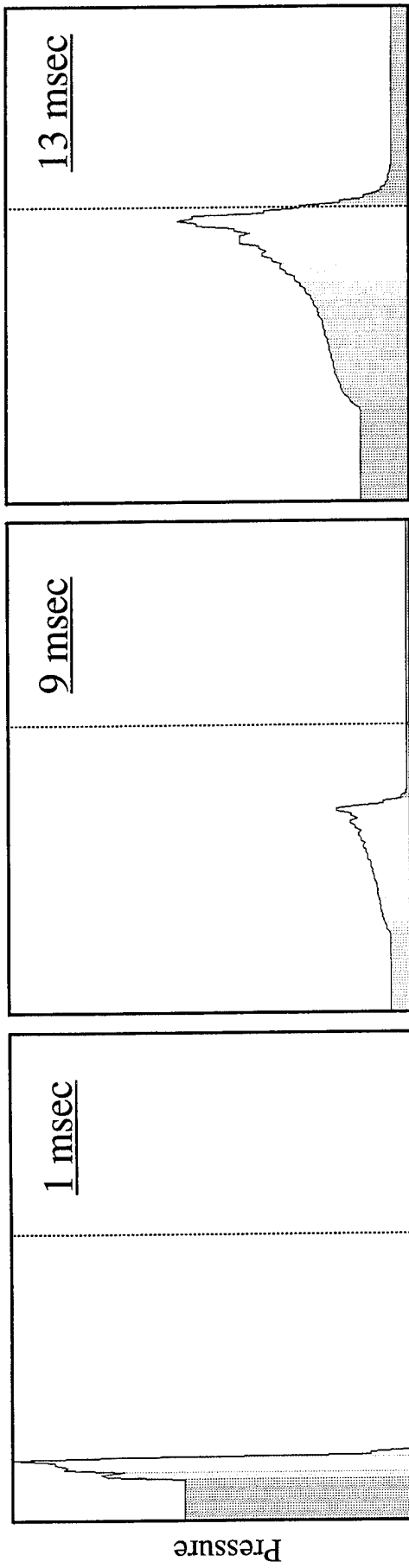
Figure 30. Snapshots of the computed pressure as a function of range in the cavity and surrounding salt medium at selected times of the 0.35 kt Azgir A2-2 simulation. The dashed vertical lines on these snapshots denote the location of the cavity wall.

57

sooner (i.e., at around 20 msec in Figure 30) and is stronger than for the previous 0.01 kt A2-4 simulation and, therefore, has a stronger influence on terminating the bubble expansion phase. The bubble then collapses to its first minimum radius of 10.5 m in about 50 msec, after which the bubble oscillations damp out to almost nothing. Thus, for this case, there is only one weak expansion/contraction cycle and a less pronounced resonance peak would be expected, in qualitative agreement with the experimental results of Figure 27.

The theoretical cavity/tamped seismic source spectral ratios corresponding to these two simulations are shown in Figure 31 where they are compared with the corresponding average observed spectral ratios from Figure 27. Here, the theoretical results have been smoothed to approximate the frequency resolution of the observations for comparison purposes. It can be seen from this figure that the theoretical simulations provide a good qualitative description of the observed differences in the seismic source characteristics of these two cavity tests. One notable discrepancy between theory and observation is that the computed resonant frequency for the 0.01 kt simulation is somewhat too high. This is perhaps not surprising, given the fact that the cavity is being approximated in the simulation as a perfect sphere, which it is not, and this might well affect the bubble period. That is, for the perfectly spherical cavity, a strong, coherent reflection is produced at the cavity wall and this reflected shock converges on the expanding gas bubble, effectively terminating its growth phase. In reality, the reflection from the actual, irregular cavity boundary could be expected to produce a less coherent reflected shock which would be less efficient at retarding the bubble growth, thereby leading to a larger bubble and longer associated bubble pulse period. Thus, given the limitations of the one-dimensional theoretical simulations described above, the degree of agreement shown in Figure 31 may be about as good as can be expected.

In any case, the evidence strongly suggests that variations in bubble pulse dynamics give rise to the most prominent yield dependent seismic source characteristics which have been identified in the data recorded from these Azgir water-filled cavity tests. While this is an interesting result, it
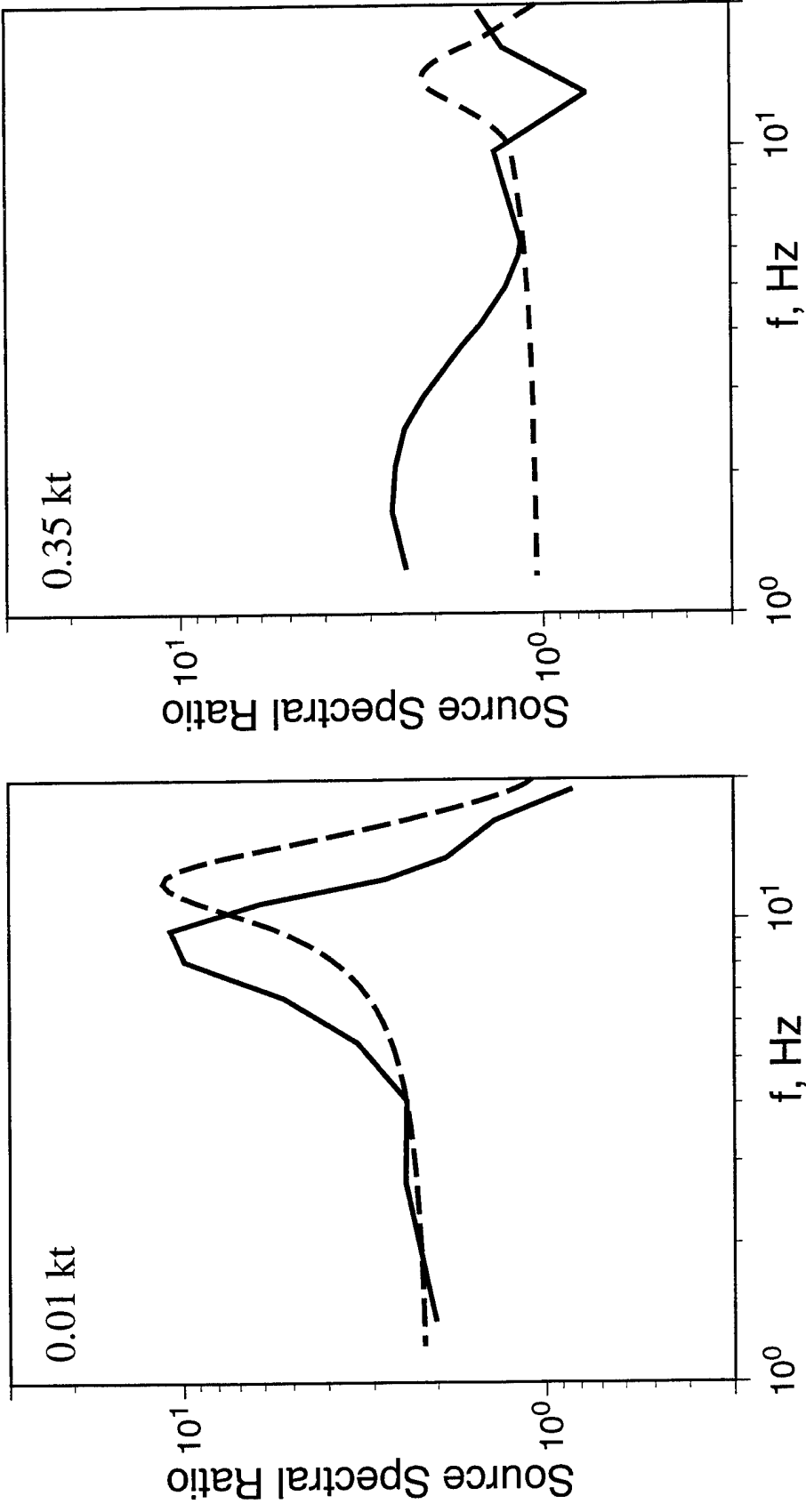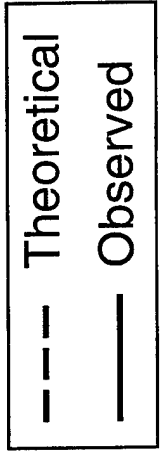
Figure 31. Comparison of observed and theoretical cavity/tamped source spectral ratios corresponding to 0.01 kt (left) and 0.35 kt (right) nuclear explosions in the Azgir water-filled cavity.

indicates that the observed seismic characteristics are dominated by the water response rather than by the response characteristics of the surrounding salt medium. Thus, it does not appear that the data recorded from these cavity tests can provide much new information which can be used to further constrain the salt equations of state to be used in theoretical simulations of the cavity decoupling evasion scenario.

4. SUMMARY AND CONCLUSIONS

4.1 Summary

It has long been recognized that the most effective means for evading the seismic detection of a clandestine underground nuclear test is to detonate the explosion in a cavity which is large enough to substantially decouple the radiated seismic signal. However, despite the fact that the feasibility of this evasion concept was experimentally established nearly 30 years ago by the U.S. STERLING nuclear cavity decoupling tests, questions still remain concerning the dependence of decoupling effectiveness on variables such as source medium, cavity size and cavity shape. This report has provided a summary of the results of a joint research program under which scientists from S-CUBED have been working with scientists from the Russian Institute for Dynamics of the Geospheres (IDG) in an attempt to develop a better understanding of the effects of different cavity decoupling variables on the seismic signals produced by underground nuclear explosions. The primary objective of this program has been to integrate available U.S. and Russian data and theoretical modeling results on cavity decoupling into an improved, quantitative model which can be used for the evaluation of the plausibility of the wide range of potential evasion scenarios which must be considered in the monitoring of any eventual CTBT.

The HE cavity decoupled test series conducted by the Russians in a uranium mine in Kirghizia in the summer of 1960 was considered in Section 2, where seismic data recorded from these tests were described and

60

analyzed. It was noted there that these decoupled tests were carried out in a variety of mined cavities in limestone, including spherical cavities having diameters ranging from about 3.5 to 10 m, as well as nonspherical cavities with volumes of about 25 m^3. The experiments of this test series consisted of 10 tamped and 12 decoupled explosions having yields of 0.1, 1.0 and 6.0 tons, and seismic data were recorded from these tests at locations in the mine over a distance range extending from about 10 to 250 m. Peak amplitudes of displacement and velocity were reported for over 250 of these recording locations and it was shown that these data provide valuable insight into the dependence of decoupling effectiveness on variables such as cavity volume, cavity shape and charge emplacement geometry. While more limited in extent, corresponding waveform data were also digitized and processed to define the frequency dependence of the observed decoupling factors.

An analysis of the seismic data recorded from a series of six nuclear explosions conducted in the same water-filled cavity at the Russian Azgir test site was presented in Section 3, where the seismic source characteristics of these explosions were studied in detail. As a result of these analyses, it was shown that the seismic signals from these explosions were not decoupled in the manner which would be expected for such explosions in air-filled cavities. On the other hand, it was noted that their wide range of energy release of over a factor of 50 in yield at a fixed detonation point does provide a unique opportunity to study the dynamic seismic response characteristics of such cavity configurations in salt. These response characteristics were systematically investigated using the results of a detailed series of finite difference simulations of these explosions in which the complex, nonlinear interactions between the shock effects in both the water and surrounding salt medium were modeled and correlated with the observed seismic data from these tests.

4.2 Conclusions

The research summarized above supports the following principal conclusions regarding the Kirghizia HE cavity decoupling test series.

(1)   Analyses of seismic data recorded from these tests indicate that HE explosions at a depth of 290 m in that limestone medium are essentially fully decoupled in spherical cavities with scaled cavity radii larger than about 27 m/kt$^{1/3}$.

(2)   Comparisons of near-field peak displacement data recorded from these tests indicate that the low frequency decoupling effectiveness is approximately independent of cavity shape for roughly cylindrical cavities with length to width ratios of 6 or more. This observed insensitivity to cavity shape is consistent with our previous theoretical simulation results.

(3)   A preliminary evaluation of seismic data recorded from tests with charge emplacements in the center of a spherical cavity and near the cavity wall suggests that close proximity of the charge to the cavity wall does lead to some enhanced nonlinear medium response, and an associated modest reduction in decoupling effectiveness.

(4)   Spectral analyses of the limited available waveform data indicate a maximum low frequency decoupling factor of about 25 for fully decoupled HE tests at this depth in the Kirghizia limestone medium. Theoretical simulation results suggest that the corresponding nuclear decoupling factor for this case would be expected to be in the range of 50-60.

With regard to the Azgir water-filled cavity tests, results of the data analysis and theoretical simulation studies support the following conclusions.

(1)   Analysis of teleseismic m_b/yield data from these explosions indicate that they were not decoupled. In fact, they seem to show enhanced coupling with respect to tamped explosions of the same yields in salt over some frequency bands, more

consistent with what would be expected for explosions in water.

(2)   Broadband seismic data recorded at near-regional distances from these explosions have been analyzed to estimate cavity/tamped source spectral ratios. These ratios show some pronounced yield dependence which appears to correlate with systematic differences in the seismic source generation mechanisms between these different explosions.

(3)   The results of theoretical finite difference simulations of nuclear explosions of different yields in this cavity indicate that the dynamic interactions between the steam bubbles generated by the explosions in the water and the shock wave reflections from the cavity wall have an important effect on the seismic source characteristics of such tests.

(4)   It is concluded that the most prominent yield dependent features which have been identified in the seismic data recorded from these tests are dominated by the water response to the explosive sources and, consequently, that these data do not provide much new information which can be used to further constrain the salt equations of state to be used in theoretical simulations of the cavity decoupling evasion scenario.

References

Adushkin, V. V., D. D. Sultanov, I. O. Kitov and O. P. Kuznetsov (1992), "Overview of the Experimental Data and Theoretical Simulations of Underground Nuclear Explosions Decoupled by large Air Filled Cavities," *Rep. Russian Acad. Sci.*, 327 (1).

Chitty, D. E., and S. E. Blouin (1993), "Laboratory Investigation of the Strength and Deformation Properties of Carbonate Rocks and Soils," DNA-TR-92-45, September.

Dobratz, B. M. (1981), "LLNL Explosives Handbook, Properties of Chemical Explosives and Explosive Simulants," LLNL Report UCRL-52997, March.

Duff, R. E., K. H. Lie, R. H. Nilson, E. W. Peterson, and N. Rimer (1987), "Late-Time Containment Research," DNA-TR-88-43, December.

Evernden, J. F. (1970), "Magnitude versus Yield of Explosions," *Journal of Geophysical Research, Vol. 75*, No. 5, p. 1028.

Glenn, L. A. and P. Goldstein (1994), "Seismic Decoupling With Chemical and Nuclear Explosions in Salt," *Journal of Geophysical Research, Vol. 99*, No. B6, p. 11,723.

Herbst, R. F., G. C., Werth and D. L. Springer (1961), "Use of Large Cavities to Reduce Seismic Waves From Underground Explosions," *J. Geophys. Res.*, 66, p. 959.

Kitov, I. O., D. D. Sultanov, V. V. Adushkin, V. N. Kostuchenko, O. P. Kuznetsov, P. B. Kaazik, N. I. Nedoshivin, H. D. Rubinshtein (1995), "Analysis of the Seismic Characteristics of U.S. and Russian Coupled

and Cavity Decoupled Explosions in Salt," Institute for the Dynamics of the Geospheres, Final Report 911412, August.

Latter, A. L., R. E. Lelevier, E. A. Martinelli and W. G. McMillan (1961), "A Method of Concealing Underground Nuclear Explosions," *J. Geophys. Res.*, *66*, p. 2929.

Lee, E., M. Finger, and W. Collins (1973), "JWL Equation of State Coefficients for High Explosives," LLNL Report UCID-16189, January.

Murphy, J. R. (1980), "An Evaluation of the Factors Influencing the Seismic Detection of Decoupled Explosions at Regional Distances," SSS-R-80-4579, July.

Murphy, J. R., J. L. Stevens and N. Rimer (1988), "High Frequency Seismic Source Characteristics of Cavity Decoupled Underground Nuclear Explosions," S-CUBED Technical Report SSS-TR-88-9595 (AFGL-TR-88-0130), ADA198121.

Murphy, J. R. and B. W. Barker (1994), "Seismic Identification Analyses of Cavity Decoupled Nuclear and Chemical Explosions," S-CUBED Technical Report SSS-TR-94-14399 (PL-TR-94-2036), ADA280947.

Murphy, J. R., I. O. Kitov, J. L. Stevens, D. D. Sultanov, B. W. Barker, N. Rimer and M. C. Friedman (1994), "Analyses of the Seismic Characteristics of U.S. and Russian Cavity Decoupled Explosions," *Rep. PL-TR-94-2295*, Phillips Laboratory, ADA292881.

Murphy, J. R., N. Rimer and J. L. Stevens (1996), 'Comments on "Seismic Decoupling With Chemical and Nuclear Explosions in Salt" by L. Glenn and P. Goldstein', *J. Geophys. Res.*, *101*, p. 346.

Pritchett, J. W. (1971), "An Evaluation of Various Theoretical Models for Underwater Explosion Bubble Pulsation," Information Research Associates Report to ARPA IRA-TR-2-71, April.

Reinke, R. E., J. A. Leverette, A. A. Martinez, D. Murrell and C. Joachim (1995), "High Explosion Decoupling Experiments in Hard Rock: The Magdalena Tests," Presentation at the Nuclear Evasion Testing Symposium, Washington, DC, January 10-12, 1995.

Rimer, N., and J. T. Cherry (1982), "Ground Motion Predictions for the Grand Saline Experiment," S-CUBED Topical Report to VELA Seismological Center, SSS-R-82-5673, VSC-TR-82-25, July.

Rimer, N., H. E. Read, S. K. Garg, S. Peyton, S. M. Day, and G. A. Hegemier (1984), "Effects of Pore Fluid Pressure on Explosive Ground Motions in Low Porosity Brittle Rocks," DNA-TR-85-245, July.

Rimer, N., T. Barker, S. Rogers, J. Stevens and D. Wilkins (1994), "Simulation of Seismic Signals from Partially Coupled Nuclear Explosions in Cylindrical Tunnels," DNA-TR-94-136, August.

Schuster, S. H., V. E. Koik, A. V. Cooper, and Y. M. Ito (1991), "Effects of EOS on Yield Estimates for Contained Explosions in Frozen Limestone," California Research and Technology Final Report to DNA CRT 3308-014F, August.

Stevens, J. L., J. R. Murphy and N. Rimer (1991a), "Seismic Source Characteristics of Cavity Decoupled Explosions in Salt and Tuff," *Bull. Seism. Soc. Am.*, *81*, pp. 1272-1291.

Stevens, J. L., N. Rimer, J. R. Murphy and T. G. Barker (1991b), "Simulation of Seismic Signals From Partially Coupled Nuclear Explosions in Spherical and Ellipsoidal Cavities," S-CUBED Technical Report SSS-FR-91-12735.

Prof. Thomas Ahrens
Seismological Lab, 252-21
Division of Geological & Planetary Sciences
California Institute of Technology
Pasadena, CA 91125

Prof. Keiiti Aki
Center for Earth Sciences
University of Southern California
University Park
Los Angeles, CA 90089-0741

Prof. Shelton Alexander
Geosciences Department
403 Deike Building
The Pennsylvania State University
University Park, PA 16802

Dr. Thomas C. Bache, Jr.
Science Applications Int'l Corp.
10260 Campus Point Drive
San Diego, CA 92121 (2 copies)

Prof. Muawia Barazangi
Cornell University
Institute for the Study of the Continent
3126 SNEE Hall
Ithaca, NY 14853

Dr. Douglas R. Baumgardt
ENSCO, Inc
5400 Port Royal Road
Springfield, VA 22151-2388

Dr. T.J. Bennett
S-CUBED
A Division of Maxwell Laboratories
11800 Sunrise Valley Drive, Suite 1212
Reston, VA 22091

Dr. Robert Blandford
AFTAC/TT, Center for Seismic Studies
1300 North 17th Street
Suite 1450
Arlington, VA 22209-2308

Dr. Stephen Bratt
ARPA/NMRO
3701 North Fairfax Drive
Arlington, VA 22203-1714

Mr. Dale Breding
Sandia National Laboratories
Organization 9236, MS 0655
Albuquerque, NM 87185

Dr. Jerry Carter
Center for Seismic Studies
1300 North 17th Street
Suite 1450
Arlington, VA 22209-2308

Mr Robert Cockerham
Arms Control & Disarmament Agency
320 21st Street North West
Room 5741
Washington, DC 20451,

Dr. Zoltan Der
ENSCO, Inc.
5400 Port Royal Road
Springfield, VA 22151-2388

Dr. Stanley K. Dickinson
AFOSR/NM
110 Duncan Avenue
Suite B115
Bolling AFB, DC 20332-6448

Dr. Petr Firbas
Institute of Physics of the Earth
Masaryk University Brno
Jecna 29a
612 46 Brno, Czech Republic

Dr. Mark D. Fisk
Mission Research Corporation
735 State Street
P.O. Drawer 719
Santa Barbara, CA 93102

Dr. Cliff Frolich
Institute of Geophysics
8701 North Mopac
Austin, TX 78759

Dr. Holly Given
IGPP, A-025
Scripps Institute of Oceanography
University of California, San Diego
La Jolla, CA 92093

Dr. Jeffrey W. Given
SAIC
10260 Campus Point Drive
San Diego, CA 92121

Dan N. Hagedon
Pacific Northwest Laboratories
Battelle Boulevard
Richland, WA 99352

1

Dr. James Hannon
Lawrence Livermore National Laboratory
P.O. Box 808, L-205
Livermore, CA 94550

Dr. Roger Hansen
University of Colorado, JSPC
Campus Box 583
Boulder, CO 80309

Prof. David G. Harkrider
Phillips Laboratory
Earth Sciences Division, PL/GPE
29 Randolph Road
Hanscom AFB, MA 01731-3010

Prof. Danny Harvey
University of Colorado, JSPC
Campus Box 583
Boulder, CO 80309

Prof. Donald V. Helmberger
Division of Geological & Planetary Sciences
California Institute of Technology
Pasadena, CA 91125

Prof. Eugene Herrin
Geophysical Laboratory
Southern Methodist University
Dallas, TX 75275

Prof. Robert B. Herrmann
Department of Earth & Atmospheric Sciences
St. Louis University
St. Louis, MO 63156

Prof. Lane R. Johnson
Seismographic Station
University of California
Berkeley, CA 94720

Prof. Thomas H. Jordan
Department of Earth, Atmospheric &
 Planetary Sciences
Massachusetts Institute of Technology
Cambridge, MA 02139

Mr. Robert C. Kemerait
ENSCO, Inc.
445 Pineda Court
Melbourne, FL 32940

U.S. Dept of Energy
Max Koontz, NN-20, GA-033
Office of Research and Develop.
1000 Independence Avenue
Washington, DC 20585

Dr. Richard LaCoss
MIT Lincoln Laboratory, M-200B
P.O. Box 73
Lexington, MA 02173-0073

Prof. Charles A. Langston
Geosciences Department
403 Deike Building
The Pennsylvania State University
University Park, PA 16802

Jim Lawson, Chief Geophysicist
Oklahoma Geological Survey
Oklahoma Geophysical Observatory
P.O. Box 8
Leonard, OK 74043-0008

Prof. Thorne Lay
Institute of Tectonics
Earth Science Board
University of California, Santa Cruz
Santa Cruz, CA 95064

Dr. William Leith
U.S. Geological Survey
Mail Stop 928
Reston, VA 22092

Mr. James F. Lewkowicz
Phillips Laboratory/GPE
29 Randolph Road
Hanscom AFB, MA 01731-3010(2 copies)

Dr. Gary McCartor
Department of Physics
Southern Methodist University
Dallas, TX 75275

Prof. Thomas V. McEvilly
Seismographic Station
University of California
Berkeley, CA 94720

Dr. Keith L. McLaughlin
S-CUBED
A Division of Maxwell Laboratory
P.O. Box 1620
La Jolla, CA 92038-1620

2

Prof. Bernard Minster
IGPP, A-025
Scripps Institute of Oceanography
University of California, San Diego
La Jolla, CA 92093

Prof. Brian J. Mitchell
Department of Earth & Atmospheric Sciences
St. Louis University
St. Louis, MO 63156

Mr. Jack Murphy
S-CUBED
A Division of Maxwell Laboratory
11800 Sunrise Valley Drive, Suite 1212
Reston, VA 22091 (2 Copies)

Dr. Keith K. Nakanishi
Lawrence Livermore National Laboratory
L-025
P.O. Box 808
Livermore, CA 94550

Prof. John A. Orcutt
IGPP, A-025
Scripps Institute of Oceanography
University of California, San Diego
La Jolla, CA 92093

Dr. Howard Patton
Lawrence Livermore National Laboratory
L-025
P.O. Box 808
Livermore, CA 94550

Dr. Frank Pilotte
HQ AFTAC/TT
1030 South Highway A1A
Patrick AFB, FL 32925-3002

Dr. Jay J. Pulli
Radix Systems, Inc.
6 Taft Court
Rockville, MD 20850

Prof. Paul G. Richards
Lamont-Doherty Earth Observatory
 of Columbia University
Palisades, NY 10964

Mr. Wilmer Rivers
Teledyne Geotech
1300 17th St N #1450
Arlington, VA 22209-3803

Dr. Alan S. Ryall, Jr.
Lawrence Livermore National Laboratory
P.O. Box 808, L-205
Livermore, CA 94550

Dr.Chandan K. Saikia
Woodward Clyde- Consultants
566 El Dorado Street
Pasadena, CA 91101

Mr. Dogan Seber
Cornell University
Inst. for the Study of the Continent
3130 SNEE Hall
Ithaca, NY 14853-1504

Secretary of the Air Force
(SAFRD)
Washington, DC 20330

Office of the Secretary of Defense
DDR&E
Washington, DC 20330

Thomas J. Sereno, Jr.
Science Application Int'l Corp.
10260 Campus Point Drive
San Diego, CA 92121

Dr. Michael Shore
Defense Nuclear Agency/SPSS
6801 Telegraph Road
Alexandria, VA 22310

Prof. David G. Simpson
IRIS, Inc.
1616 North Fort Myer Drive
Suite 1050
Arlington, VA 22209

Dr. Jeffrey Stevens
S-CUBED
A Division of Maxwell Laboratory
P.O. Box 1620
La Jolla, CA 92038-1620

Prof. Brian Stump
Los Alamos National Laboratory
EES-3
 Mail Stop C-335
Los Alamos, NM 87545

3

Prof. Tuncay Taymaz
Istanbul Technical University
Dept. of Geophysical Engineering
Mining Faculty
Maslak-80626, Istanbul Turkey

Prof. M. Nafi Toksoz
Earth Resources Lab
Massachusetts Institute of Technology
42 Carleton Street
Cambridge, MA 02142

Dr. Larry Turnbull
CIA-OSWR/NED
Washington, DC 20505

Dr. Karl Veith
EG&G
2341 Jefferson Davis Highway
Suite 801
Arlington, VA 22202-3809

Prof. Terry C. Wallace
Department of Geosciences
Building #77
University of Arizona
Tuscon, AZ 85721

Dr. William Wortman
Mission Research Corporation
8560 Cinderbed Road
Suite 700
Newington, VA 22122

ARPA, OASB/Library
3701 North Fairfax Drive
Arlington, VA 22203-1714

HQ DNA
ATTN: Technical Library
Washington, DC 20305

Defense Technical Information Center
8725 John J. Kingman Road
Ft Belvoir, VA 22060-6218(2 copies)

TACTEC
Battelle Memorial Institute
505 King Avenue
Columbus, OH 43201 (Final Report)

Phillips Laboratory
ATTN: GPE
29 Randolph Road
Hanscom AFB, MA 01731-3010

Phillips Laboratory
ATTN: TSML
5 Wright Street
Hanscom AFB, MA 01731-3004

Phillips Laboratory
ATTN: PL/SUL
3550 Aberdeen Ave SE
Kirtland, NM 87117-5776 (2 copies)

Dr. Michel Campillo
Observatoire de Grenoble
I.R.I.G.M.-B.P. 53
38041 Grenoble, FRANCE

Dr. Kin Yip Chun
Geophysics Division
Physics Department
University of Toronto
Ontario, CANADA

Prof. Hans-Peter Harjes
Institute for Geophysic
Ruhr University/Bochum
P.O. Box 102148
4630 Bochum 1, GERMANY

Prof. Eystein Husebye
IFJF
Jordskjelvstasjonen
Allegaten, 5007 BERGEN NORWAY

David Jepsen
Acting Head, Nuclear Monitoring Section
Bureau of Mineral Resources
Geology and Geophysics
G.P.O. Box 378, Canberra, AUSTRALIA

Ms. Eva Johannisson
Senior Research Officer
FOA
S-172 90 Sundbyberg, SWEDEN

Dr. Peter Marshall
Procurement Executive
Ministry of Defense
Blacknest, Brimpton
Reading FG7-FRS, UNITED KINGDOM

4

Dr. Bernard Massinon, Dr. Pierre Mechler
Societe Radiomana
27 rue Claude Bernard
75005 Paris, FRANCE (2 Copies)

Dr. Svein Mykkeltveit
NTNT/NORSAR
P.O. Box 51
N-2007 Kjeller, NORWAY (3 Copies)

Dr. Jorg Schlittenhardt
Federal Institute for Geosciences & Nat'l Res.
Postfach 510153
D-30631 Hannover , GERMANY

Dr. Johannes Schweitzer
Institute of Geophysics
Ruhr University/Bochum
P.O. Box 1102148
4360 Bochum 1, GERMANY

Trust & Verify
VERTIC
Carrara House
20 Embankment Place
London WC2N 6NN, ENGLAND